Title: The influence of soil temperature and water content on belowground hydraulic conductance and leaf gas exchange in mature trees of three boreal species

Authors: Anna Lintunen[1,2], Teemu Paljakka[2], Yann Salmon[1,2], Roderick Dewar[1,3], Anu Riikonen[2], Teemu Hölttä[2]

[1] Institute for Atmospheric and Earth System Research / Physics, Faculty of Science, University of Helsinki, P.O. Box 68, FI-00014 Helsinki, Finland

[2] Institute for Atmospheric and Earth System Research / Forest Sciences, Faculty of Agriculture and Forestry, University of Helsinki, P.O. Box 27, FI-00014 Helsinki, Finland

[3]Plant Sciences Division, Research School of Biology, The Australian National University, Canberra ACT 2601, Australia

Contact information for correspondence:

Anna Lintunen

E-mail: anna.lintunen@helsinki.fi

Phone: +358 40 7510341

Funding:

The work was funded by the Academy of Finland grants no. 310375, 307331, and the Finnish Cultural Foundation grant no. 00180821.

Conflict of Interest Statement:

The authors declare that there are no conflicts of interest.

Abstract

Understanding stomatal regulation is fundamental to predicting the impact of changing environmental conditions on vegetation. However, the influence of soil temperature (ST) and soil water content (SWC) on canopy conductance (g_s) through changes in belowground hydraulic conductance (k_{bg}) remains poorly understood, because k_{bg} has seldom been measured in field conditions. Our aim was to i) examine the dependence of k_{bg} on ST and SWC, ii) examine the dependence of g_s on k_{bg}, and iii) test a recent stomatal optimization model according to which g_s and soil-to-leaf hydraulic conductance are strongly coupled. We estimated k_{bg} from continuous sap flow and xylem diameter measurements in three boreal species. k_{bg} increased strongly with increasing ST when ST was below +8 °C, and typically increased with increasing SWC when ST was not limiting. g_s was correlated with k_{bg} in all three species, and modelled and measured g_s were well correlated in *Pinus sylvestris* (a model comparison was only possible for this species). These results imply an important role for k_{bg} in mediating linkages between the soil environment and leaf gas exchange. In particular, our finding that ST strongly influences k_{bg} in mature trees may help us to better understand tree behaviour in cold environments.

Key words: belowground hydraulic conductance, cold, point dendrometer, sap flow, stomatal control, water relations

Summary statement: Soil temperature and water content are important factors influencing belowground hydraulic conductance and canopy conductance in mature boreal trees.

Introduction

For high latitude forests, air temperatures are expected to increase two-fold compared to the global average change of temperature (IPCC 2018). When combined with a decrease in the depth and duration of insulating snow cover, important changes in soil temperature may be expected (Aalto, Scherrer, Lenoir, Guisan & Luoto, 2018). The effect of soil temperature on tree or stand level gas exchange and carbon uptake remains poorly understood, and thus poorly represented in models, despite the important role of soil temperature in high latitude ecosystem functioning (Aalto et al, 2018; Niittynen, Heikkinen & Luoto, 2018). For example, the fact that current biosphere models overestimate springtime photosynthesis and gross primary production in boreal coniferous forests (Böttcher et al, 2016) may reflect their failure to take into account important linkages between soil temperature and tree gas exchange.

Plants absorb CO_2 for photosynthesis through leaf stomatal pores. The cost of CO_2 absorption through the stomata is the concurrent loss of water to the atmosphere, so that these two processes are tightly coupled. The water lost from leaves is replaced by water uptake from the soil and sap flow through the xylem. Stomatal conductance and photosynthesis are known to decrease sharply when soil temperature is decreased below approximately +8 °C in boreal conifers (Day, Heckathorn & DeLucia, 1991; DeLucia, 1986; Lippu & Puttonen, 1991; Mellander, Bishop & Lundmark, 2004). Under these conditions, insufficient water is available for trees because cold soil limits the capacity of trees to extract water from the soil, thus reducing transpiration and photosynthesis.

The linkage between soil temperature and tree gas exchange may occur through changes in belowground hydraulic conductance (k_{bg}), i.e. hydraulic conductance from bulk soil to stem base. And yet k_{bg} is one of the least understood components of the water transport pathway from the soil to leaves. k_{bg} has been measured in the laboratory for smaller plants (e.g. BassiriRad, Radin & Matsuda, 1991; Nobel, Schulte & North, 1990; Running & Reid, 1980) and tree seedlings of various species

71 (e.g. Day *et al.*, 1991; Cochard, Martin, Gross & Bogeat-Triboulot, 2000; McLean, Ludwig &
72 Grierson, 2011; Wan, Landhäusser, Zwiazek & Lieffers, 1999; Wan, Zwiazek, Lieffers &
73 Landhäusser, 2001), but it has seldom been measured continuously for mature trees in field conditions
74 (but see Martínez-Vilalta, Korakaki, Vanderklein & Mencuccini, 2007; McElrone et al, 2007;
75 Poyatos, Aguadé & Martínez-Vilalta, 2018 for rare examples of such studies). As far as we are aware,
76 the preliminary study by Lintunen et al. (2018) is the only one to have monitored the belowground
77 hydraulic conductance of mature trees in conditions where soil temperature is limiting.

78 Hydraulic conductance affects stomatal conductance indirectly through its effects on leaf water
79 potential (Comstock & Mencuccini, 1998; Mellander et al, 2004). On theoretical grounds, a recent
80 optimization model of stomatal conductance (Dewar et al, 2018; Hölttä et al, 2017) predicts that g_s is
81 approximately proportional to the square root of soil-to-leaf hydraulic conductance (k_{sl}), of which k_{bg}
82 is a key component. This model, which provides a theoretical framework for the design of the present
83 study, is based on the hypothesis that g_s varies to maximize photosynthesis, where the cost of stomatal
84 opening occurs through non-stomatal limitations to photosynthesis induced by decreased leaf water
85 potential or increased leaf sugar concentration (Friend, 1991; Givnish, 1986; Hölttä et al, 2017). The
86 model offers testable predictions for the cost associated with non-stomatal limitations to
87 photosynthesis (Gimeno, Saavedra, Ogée, Medlyn & Wingate, 2019) as well as for the close coupling
88 between g_s and soil-to-leaf hydraulic conductance.

89 Hydraulic conductance is defined as the flow rate per unit pressure driving force (Nobel 2009). In the
90 case of belowground hydraulic conductance, the driving force is the water potential difference
91 between the bulk soil and stem base. Martínez-Vilalta et al (2007) introduced an approach where k_{bg}
92 is calculated as the ratio of sap flow rate to the difference between soil and stem base water potentials,
93 where the latter are estimated from xylem diameter measurements conducted at the stem base at
94 predawn and during the day, respectively. This approach is based on the observation that tree stems

shrink in diameter during the day and swell during the night in response to changes in water tension in the xylem, and the shrinkage can easily be measured in a nondestructive way to derive continuous information about tree water potential (Alméras, 2008; Alméras & Gril, 2007; Irvine & Grace, 1997; Perämäki et al, 2001). Under steady-state conditions, various studies have found a linear correlation between reversible changes in xylem or whole stem diameter (corrected for growth if required) and changes in xylem water potential (Badal et al, 2010; Cochard, Forestier & Améglio, 2002; Intrigliolo et al, 2011; Irvine & Grace 1997; Ortuño et al, 2006; Ueda & Shibata, 2001). The approach of Martínez-Vilalta et al. (2007) was recently used to study belowground hydraulic constraints during drought-induced decline in *Pinus sylvestris* in a Mediterranean climate (Poyatos et al, 2018), and was also tested with one *P. sylvestris* tree in a boreal environment (Lintunen et al, 2018).

In this study, our overall objective was to test the hypothesis that belowground hydraulic conductance (k_{bg}) is an important link between soil conditions and leaf gas exchange. We examined k_{bg} and its linkage to canopy conductance (g_s) in mature *P. sylvestris* trees growing in a boreal forest stand, and in *A. glutinosa* and *T. x vulgaris* trees growing in a boreal urban environment in Southern Finland. These three case studies were selected in order to study mature trees in their natural growth environment (forest stand) and trees in a more extreme growth environment (urban sites). Within this overall objective, our first aim was to examine how k_{bg} depends on soil temperature and soil water content in a coniferous species in a forest stand over several growing seasons, and in broadleaved species in an urban environment over a growing season. We hypothesize that soil temperature has a strong effect on k_{bg} in boreal environments. Our second aim was to examine how g_s is linked to k_{bg}, and specifically, to compare observed g_s in *P. sylvestris* with g_s predicted by the stomatal optimization model (Dewar et al, 2018; Hölttä et al, 2017) according to which g_s is closely coupled to the soil-to-leaf hydraulic conductance.

Material and methods

A list of symbols, their definitions and units is given in Table 1.

Study site

We measured three *Pinus sylvestris* (L.) trees in a boreal, evergreen coniferous forest at SMEAR II station in Hyytiälä (N 61˚ 50.8' , E 24˚ 17.7', 180 m.a.s.l.), Finland: tree 1 in year 2016, trees 1 and 2 in year 2015, and tree 3 in year 2013. The average height of the measured trees in the measurement year was 18 m and average breast height diameter was 20 cm. The trees were 54 years old in year 2016. The vegetation type is *Vaccinium* (Cajander, 1949) and the forest floor is dominated by dwarf shrubs and mosses. The soil type is glacial till, which is the most common soil type in Finland. Annual precipitation is 700 mm and average air temperature +4 °C.

In the urban environment, we measured three *Alnus glutinosa* (L.) Gaertn. f. *pyramidalis* 'Sakari' trees in 2010, one *Tilia* × *vulgaris* Hayne tree in year 2012, and two *Tilia* trees in year 2013. The trees were planted in 2002 on two separate streets in the city of Helsinki, Finland. The growing media consisted of pre-mixed structural soil, and the soil plot dimensions for each tree were 3 m wide with 1 m deep strips placed within the standard load bearing gravel of the street. The spacing for *A. glutinosa* was 4-5 m and for *T. x vulgaris* 15 m, and subsurface drains were installed on both streets. The level of the water table at the *T. x vulgaris* site was continuously high due to water being collected from a larger catchment area compared to the *A. glutinosa* site, which received only local rainfall. The average tree height and breast height diameter in the sites in 2010 were 11 m and 15 cm, respectively for *Alnus*, and 6 m and 13 cm, respectively for *T. x vulgaris*. Details of the research sites, soils and street surfacing are given in Riikonen et al (2011) and Riikonen et al (2016). Annual precipitation is 680 mm and average air temperature +5 °C.

Field measurements

142 Sap flux density was measured with a constant heat dissipation sensor (Granier, 1985). Pairs of 4 cm
143 probes (typical conductive depth of sapwood in mature pine trees at SMEAR II station) were inserted
144 into the xylem at a height of 1.3 m in *P. sylvestris* and 0.5-1 m in *A. glutinosa* and *T. x vulgaris*. The
145 vertical separation of the sensors was 10 cm, and they were covered with a reflective aluminum
146 shelter. The sensors were located on the northern side of the stem. Sap flux density was recorded
147 every minute. Zero sap flux density at night was defined as the average of seven consecutive nights
148 as suggested by Lu et al (2004). Sap flow rate was calculated from the sap flux density multiplied by
149 the leaf area. Leaf area for each tree was estimate by multiplying the conductive sapwood area with
150 leaf to sap wood area ratio of 2000 m^2 m^{-2} (Martínez-Vilalta et al, 2009).

151 The water potential difference between the bulk soil and stem base was derived from xylem diameter
152 measurements (*P. sylvestris* at breast height, *A. glutinosa* and *T.* x *vulgaris* at 20-40 cm height).
153 Xylem diameter was continuously measured with linear displacement transducer point dendrometers
154 (Solartron Inc., Model AX/5-0/5, Bognor Regis, West Sussex, UK; accuracy of 1 μm). The
155 measurement apparatus has a negligible thermal expansion (Sevanto et al, 2005a) because thermal
156 expansion of the frame and wood nearly compensate each other. Because the thermal expansion
157 coefficient of wood is not exactly known, diameter changes were not corrected for thermal expansion;
158 a sensitivity analysis of the effect of various corrections for wood thermal expansion showed no
159 significant effect on our overall conclusions (data not shown). Air temperature and photosynthetic
160 active radiation (PAR) were continuously measured at a height of 16 m at the SMEAR II station and
161 8 m at the urban sites, and soil temperature and volumetric water content in the B1 horizon in 9-14
162 cm depth at all sites (see Hari & Kulmala, 2005; Riikonen, Järvi & Nikinmaa, 2016). The B1 horizon
163 was selected because daily maximum transpiration has been shown to be most closely linked to the
164 water content of soil deeper than 5 cm at the studied forest site (Duursma et al, 2008). At the SMEAR
165 II site, relative air humidity was measured locally, adjacent to air temperature; for the urban sites, we
166 used air humidity measured at the nearby (4 km) SMEAR III urban measurement station (Järvi et al,

167 2009). Vapor pressure deficit (*D*) was calculated from air humidity and air temperature
168 measurements.

169 Stem water potential was assumed to be linearly proportional to the instantaneous xylem diameter
170 (e.g. Irvine & Grace, 1997; Perämäki et al, 2001). This assumption has been empirically verified by
171 numerous studies for various conifer and broadleaved species (e.g. Cochard et al, 2002; Dietrich,
172 Zweifel & Kahmen, 2018; Irvine & Grace, 1997; Offenthaler, Hietz & Richter, 2001; Ueda & Shibata,
173 2001). We also tested the relationship by measuring stem water potential and xylem diameter from
174 *A. glutinosa* in the morning, mid-day and afternoon for 5 days in June 2011 (R^2=0.73, Fig. **1a**). If
175 water potential drops below the species-specific cavitation threshold, the assumption of linear
176 relationship between water potential and xylem diameter is violated as cavitation releases water
177 tension so that the tissue swells (Alméras 2008; Dietrich et al, 2018; Offenthaler et al, 2001; Rosner,
178 Karlsson, Konnerth & Hansmann, 2009; Rosner, Konnerth, Plank, Salaberger & Hansmann, 2010).
179 In the studied boreal climate, however, the cavitation thresholds can be expected to be reached only
180 rarely, at least for pine (Hölttä et al, 2005; Sevanto et al, 2005b).

181 When soil water potential (ψ_s) differed significantly from zero, maximum xylem diameter (dx_{max})
182 measured during night-time was used as a proxy for ψ_s assuming: 1) that both variables are linearly
183 related, in agreement with earlier studies (Martínez-Vilalta et al, 2007; Meng et al, 2017; de Santana,
184 de Almeida Bocate, Sgobi, Borges Valeriano & de Souza, 2017); and 2) that predawn xylem water
185 potential is in equilibrium with ψ_s (Bréda, Granier, Barataud & Moyne, 1995; Ĉermák, Huzulák &
186 Penka, 1980; Fahey & Young, 1984; Garnier & Berger 1987; Sala, Lauenroth, Parton & Trlica, 1981).
187 To test the first assumption, we compared the concurrently measured dx_{max} and ψ_s at the *Pinus* forest
188 site in May-August 2015. ψ_s was measured every 15 minutes from the B1 horizon with an
189 equitensiometer (EQ2, Delta-T Devices, Cambridge, UK). ψ_s and dx_{max} were linearly correlated
190 (R^2=0.85, Fig. **1b**). The second assumption would be violated in the case of nocturnal transpiration,
191 as has been the case in some earlier studies (see Donovan, Linton & Richards, 2001), but in that case,

192 the assumption of zero sap flux density during the night would have the same error (i.e. nocturnal sap
193 flow would produce artificially lower dx_{max} and daily maximum sap flow rate (F_{max})) and thus the
194 errors would cancel each other in the calculation of k_{bg}.

195 When ψ_s was close to zero, dx_{max} was always assumed to represent predawn xylem water potential
196 (in equilibrium with ψ_s) even if dx_{max} changed independently of ψ_s. This assumption was made
197 because other mechanisms than changes in xylem water potential, such as changes in osmotic content
198 in the living cells of the xylem or changes in resin content (Rissanen et al, 2016), might have induced
199 changes in dx_{max} during these periods. This assumption, however, does not bias the interpretation of
200 our results, because these other mechanisms would equally affect dx_{max} and the minimum diurnal
201 diameter (dx_{min}), and thus do not affect their difference, on which our study is based.

202 It was assumed here that internal water stores did not play a role in stem diameter changes on a daily
203 scale. It is likely that there is some scatter in the results due to this assumption, but we minimized the
204 influence of diurnal capacitance effects and time lags between variables by using maximum daily
205 values instead of hourly values (Martínez-Vilalta et al, 2007).

206 Rainy and very humid days (when the daily mean of the 10% lowest values of relative humidity was
207 above 75%), and days with freezing events (when the daily mean of the 10% lowest values of ambient
208 air temperature was below 0 °C) were excluded from the analysis. We excluded rainy days because
209 water uptake directly through the bark may interfere with the interpretation of the xylem diameter
210 change measurements, and the thermal dissipation method for measuring sap flux density is known
211 not to be accurate in low flow conditions (e.g. Hölttä, Linkosalo, Riikonen, Sevanto & Nikinmaa,
212 2015). Days with a minimum temperature below zero were excluded because freezing causes artefacts
213 in both diameter change (Lindfors et al, 2015; Lintunen et al, 2015) and sap flux density
214 measurements. Additionally, days when broadleaves had no leaves were excluded for *A. glutinosa*
215 and *T.* x *vulgaris*, because the sap flux density signal is too low for reliable detection on those days.

We also excluded days before leaf area reached 15% of its total, and after leaf fall had reached 70% (see Riikonen et al, 2016 for leaf area measurement method).

Empirical calculation of belowground hydraulic conductance and canopy conductance

A daily diameter-based measure of belowground hydraulic conductance ($k_{bg,d}$) was calculated as the ratio of the daily maximum (mean of the 10 % highest values) flow rate (F_{max}, i.e. sap flux density multiplied by leaf area) to the difference between the daily maximum ($dx_{max,}$ mean of the 10% highest values) and daily minimum ($dx_{min,}$ mean of the 10% lowest values) xylem diameters (Fig. **2**). As noted above, we calculated daily values because time lags caused by hydraulic capacitance likely disturb analysis of shorter-term dynamics (Martínez-Vilalta et al, 2007). The $k_{bg,d}$ values thus obtained were then divided by their maximum value per tree per growing season, to obtain a seasonally normalized (fractional) daily belowground hydraulic conductance value f_{bg} lying between 0 and 1. Because of normalization, f_{bg} can be considered independent of leaf area and so can be calculated directly from sap flux density (l m^{-2} h^{-1}). The value of $k_{bg,d}$ was only calculated when soil temperature started to increase from zero, corresponding to the time of soil thawing. Daily maximum canopy conductance (g_s) was calculated as the ratio of the daily maximum value of sap flux density to the daily maximum (mean of the 10% highest values) D (Fig. **2**).

Linking belowground hydraulic conductance and canopy conductance: an optimization model

We used the analytical solution of the optimal stomatal conductance model derived by Dewar et al (2018) to predict a relationship between belowground hydraulic conductance (k_{bg}) and canopy conductance (g_s). The optimal stomatal conductance model is a leaf-level model which assumes infinite boundary layer conductance; therefore, in comparing the model with measured canopy-level conductance we are assuming the canopy is a homogeneous crown that is well-coupled to the atmosphere. The basic assumption of the optimization hypothesis is that g_s maximizes the rate of leaf

239 photosynthesis, where the cost of stomatal opening occurs through non-stomatal limitation (NSL) to
240 leaf photosynthesis induced by lower leaf water potential. We applied this hypothesis to a simple bi-
241 substrate model of leaf photosynthesis (A, mol m^{-2} s^{-1}) as a function of photosynthetically active
242 radiation (Q, mol m^{-2} s^{-1}) and intercellular CO_2 concentration (c_i, mol mol^{-1}), in which both the initial
243 slope (carboxylation efficiency) and plateau (carboxylation capacity) of the A-c_i curve are subject to
244 NSL (Dewar et al, 2018, Case 1 in their Table 1). The analytical solution for g_s (Dewar et al, 2018,
245 their Table 3; see also Supporting Information) is given by

246 $$g_s = \frac{\alpha_0 Q}{a_0 Q r_{x,0} + 2\Gamma^*} \frac{1-\psi_s/\psi_c}{\sqrt{z}} \left[\frac{1+\sqrt{z}}{(1+\sqrt{z})^2 + w} \right] \quad (1)$$

247 where α_0 (mol mol^{-1}) and $r_{x,0}$ (mol^{-1} m^2 s) are, respectively, the photosynthetic quantum yield and
248 carboxylation resistance in the absence of NSL, Γ* is the CO_2 photorespiratory compensation point
249 (mol mol^{-1}), ψ_s is the soil water potential (MPa), ψ_c is the critical leaf water potential (MPa) at which
250 NSL reduces leaf photosynthesis to zero, and z and w are the dimensionless parameter combinations

251 $$z = \frac{\alpha_0 Q}{a_0 Q r_{x,0} + 2\Gamma^*} \frac{1.6D}{k_{sl}|\psi_c|} \quad (2)$$

252 and

253 $$w = \frac{c_a - \Gamma^*}{a_0 Q r_{x,0} + 2\Gamma^*} \quad (3)$$

254 in which D is the atmospheric water vapour pressure deficit (mol mol^{-1}), k_{sl} is the soil-to-leaf hydraulic
255 conductance (mol m^{-2} s^{-1} MPa^{-1}), and c_a is the atmospheric CO_2 concentration (mol mol^{-1}).

256 The dependence of g_s on k_{sl} occurs through the parameter combination z (eqn 2). In order to link g_s to
257 belowground hydraulic conductance (k_{bg}), we assumed here that, within a growing season, variation
258 in the soil-to-leaf hydraulic conductance (k_{sl}) is dominated by variation in k_{bg}, because *P. sylvestris*
259 at SMEAR II station has been shown to experience drought-induced embolism only marginally

(Hölttä et al, 2005; Sevanto et al, 2005b). Total hydraulic conductance from soil to leaf (k_{sl}) was modelled as a variable hydraulic conductance from soil to stem base (k_{bg}) connected in series to a constant hydraulic conductance from stem base to leaf (k_{rl}), i.e.

$$\frac{1}{k_{sl}} = \frac{1}{k_{bg}} + \frac{1}{k_{rl}} \quad (4)$$

The variation of k_{bg} within each year and tree was expressed by writing k_{bg} as the annual maximum hydraulic conductance ($k_{bg,max}$) multiplied by the fractional or normalized value (f_{bg}) that varied between 0 and 1,

$$k_{bg} = k_{bg,max}\ f_{bg} \quad (5)$$

where f_{bg} was calculated from xylem diameter measurements as described above. We assumed that the constant hydraulic conductance from the stem base to the leaf was equal to the maximum value of the belowground hydraulic conductance,

$$k_{rl} = k_{bg,max} \quad (6)$$

This partitioning between below- and above-ground conductances is in agreement with earlier studies of Scots pine trees (Martínez-Vilalta et al, 2007). Combining eqns (4)-(6) and rearranging then gives

$$k_{sl} = k_{bg,max}\left(\frac{f_{bg}}{f_{bg}+1}\right) \quad (7)$$

The constant $k_{bg,max}$ was chosen to be 0.00066 mol m^{-2} s^{-1} MPa^{-1} so that the maximum k_{sl} (corresponding to f_{bg} = 1) was 0.00033 mol m^{-2} s^{-1} MPa^{-1} (so that minimum leaf water potential would be -3MPa when calculated from sap flow rate and k_{sl}).

Eqn (7) was then used to substitute for k_{sl} in the expression for the stomatal parameter z (eqn 2). It may be shown from eqns (1)-(3) that the predicted dependence of g_s on f_{bg} is given approximately by (see in more detail from Supporting Information)

$$g_s \approx C\sqrt{\left(\frac{f_{bg}}{f_{bg}+1}\right)} \quad (8)$$

where the parameter C (with dimensions of g_s), given by

$$C = \frac{1-\psi_s/\psi_c}{1+w}\sqrt{\frac{\alpha_0 Q}{a_0 Q r_{x,0}+2\Gamma^*}\frac{|\psi_c|k_{bg,max}}{1.6D}}, \quad (9)$$

depends on environmental conditions. Eqns (8) and (9) predict that g_s is an increasing function of f_{bg}, and that the sensitivity of g_s to changes in f_{bg} increases with increasing C, corresponding to environmental conditions that favor stomatal opening (e.g. less negative soil water potential, higher light, lower D).

For D and Q, daily maximum values (mean of 10 % highest values) were used. The values for the photosynthetic parameter $r_{x,o}$ (2 mol^{-1} m^2 s) and the CO_2 photorespiratory compensation point Γ* (40 x 10^{-6} mol mol^{-1}) were taken from Hölttä et al (2017). The value for ψ_c (-3.75 MPa) for *P. sylvestris* in boreal conditions were taken from Hölttä et al (2017).

In order to estimate photosynthetic parameters required for the stomatal optimization model, shoot gas exchange was measured continuously with automatically opening and closing chambers from one selected shoot from two of the measured *P. sylvestris* trees. Data for photosynthetic quantum yield (α) was derived during a three-day interval from midday gas exchange measurements using a fixed-curvature light response curve (Kolari, Lappalainen, Hänninen & Hari, 2007; Aalto et al, 2015), and α_0 on each day was estimated from the daily leaf water potential ($\psi_l = \frac{-F_{max}}{k_{sl}\,A_{leaf}}$ where F_{max} is sap flow

298 rate and A_{leaf} is leaf area) to be $\alpha_0 = \alpha\left(1 - \frac{\psi_l}{\psi_c}\right)^{-1}$ in accordance with the assumption of NSL in the
299 stomatal optimization model (Dewar et al, 2018). For the days in between, α_0 was interpolated
300 assuming a linear relation between the existing points. Data for α_0 was not available for year 2013.

301 Statistical analysis

302 First, we analyzed how soil temperature, soil water content and their interaction affect normalized
303 values of k_{bg} (i.e. f_{bg}) in different species. In addition, for the evergreen species *P. sylvestris* the effect
304 of season and its interaction with soil temperature and water content were included in the analysis.
305 For the broadleaved species *A. glutinosa* and *T. x vulgaris*, the data mainly consisted of summertime
306 values due to leafless spring and autumn. The seasons were defined so that spring begins when soil
307 temperature starts to increase from 0 °C, corresponding to the time of snow thawing, and continues
308 until the soil temperature reaches +8 °C. Then summer follows and continues until the soil
309 temperature drops again below +8 °C, after which it is autumn until the daily minimum (mean of 10%
310 lowest values) ambient temperature drops below 0 °C. +8 °C was selected as a boundary value
311 because of the obvious change in the relationship between soil temperature and k_{bg} at this temperature.
312 Also previous literature suggests that canopy conductance and photosynthesis decrease sharply in
313 seedlings when soil temperature is decreased below +8 °C or +10 °C in boreal environment (Day et
314 al, 1991; DeLucia, 1986; Lippu & Puttonen, 1991; Mellander et al, 2004).

315 The analysis on how k_{bg} was affected by soil environmental variables was performed independently
316 for each tree species. We used a mixed effect model with restricted maximum likelihood method in
317 the MIXED procedure in Statistical Analysis System (SAS, version 9.4, SAS Institute Inc., Cary,
318 USA; Table **2**). For each species, all data were analyzed together using normalized values of k_{bg} (i.e.
319 f_{bg}) per tree per year and repetitive measurements within a tree per year were treated with covariance
320 parameter as a random effect. First, we analyzed the effect of soil temperature, season and their
321 interaction on f_{bg} (Table **2A**), then the effect of soil water content, season and their interaction on f_{bg}

322 (Table **2B**), and finally a model with all fixed effects was introduced: soil temperature, soil water
323 content, season, and interactions: season * soil temperature and season * soil water content (Table
324 **2C**). Akaike's Information Criteria (AIC) was used for model selection. The number of observations
325 (daily values) used was 471, 401 and 396, for *P. sylvestris*, *A. glutinosa* and *T. x vulgaris*, respectively.

326 Secondly, we examined the relationship between normalized canopy conductance ($g_{s,norm}$, defined as
327 g_s divided by its seasonal maximum value), f_{bg}, season and their interaction variable (Table **3**).
328 Analyses were made with a mixed effect model in the MIXED procedure in SAS. We used log-
329 transformed values in the statistical analysis, because the data had a power-law form. The random
330 effect and model selection (in case of pine; weather the season was included in the final model or not)
331 were similar as described above and the number of observations used was 469, 401 and 396, for *P.*
332 *sylvestris*, *A. glutinosa* and *T. x vulgaris*, respectively. Because both g_s and f_{bg} are calculated from sap
333 flux density, and are thus statistically correlated, we calculated a corrected r^2 value as the square of
334 the partial coefficient of correlation, i.e. r^2 of g_s and f_{bg} after the normalized sap flux density has been
335 partialed out from them both (Table **3**). More generally, the square of the partial coefficient of
336 correlation between *Y* and *X* after having eliminated the effect of *Z* from both of them, is given by
337 (Shipley, 2016)

338 $$r^2{}_{(Y.X|Z)} = \frac{(r_{Y.X} - r_{Y.Z}\, r_{X.Z})^2}{(1 - r^2{}_{Y.Z})(1 - r^2{}_{X.Z})} \qquad (10)$$

339 where *Y*, *X* and *Z* are dependent variables, and e.g. $r_{Y,X}$ is the coefficient of correlation of *Y* and *X*.
340 First, *Y* is predicted from *Z* and *X* is predicted from *Z*. Second, the residuals of these predictions are
341 computed and correlated.

342 Finally, we used a mixed model (SAS) to examine how well the measured and modelled canopy
343 conductance correlate with each other (Table **3**). The random effect was similar as described for Table
344 1. This analysis was only done for *P. sylvestris* as we did not have photosynthetic data for *A. glutinosa*

and *T. x vulgaris*. The measured and modelled g_s were treated in the analysis as independent of each other, because although sap flux density played a large role in calculating the measured g_s (r^2 = 0.22 for linear dependency between g_s and sap flux density, not shown), the statistical correlation between sap flux density and the modelled g_s was numerically small (r^2 = 0.02, not shown), due to the algebraic form of the dependence of modelled g_s on f_{bg} given by eqn 8, and to the presence of other sources of variation in modelled g_s via the environmental factor C in eqn 8. The number of observations used for *P. sylvestris* was 319 (photosynthetic measurement data available for years 2015 and 2016).

Results

Sap flow rate, xylem diameter change amplitude, daily maximum vapor pressure deficit, soil temperature and normalized belowground hydraulic conductance (f_{bg}) increased from spring towards the summer and decreased again in autumn in the three studied cases (Figs. **3, 4, 5**). Soil water content increased in spring, was lowest in summer and increased again in autumn in all studied years and sites (Fig. **3, 4, 5**). However, the decrease in soil water content in the wet urban site for *T.* x *vulgaris* was more limited than for the other species even during the summer months (Fig. **5**). f_{bg} did not decrease below 0.2, and was seldom below 0.3 in summer (Fig. **3, 4, 5**). However, the *A. glutinosa* trees showed a decrease in f_{bg} during the warmest and driest summer month (Fig. **4**), which was not seen in evergreen *P. sylvestris* trees growing in a forest (Fig. **3**) or in *T. x vulgaris* street trees measured on wet urban site (Fig. **5**).

f_{bg} of *P. sylvestris* increased with increasing soil temperature in all seasons (Table **2a**, Fig. **6a**). In summer, f_{bg} increased with increasing soil water content, but the correlation between f_{bg} and soil water content was negative in spring and autumn (Table **2b**, Fig. **7a**). This is because f_{bg} increased with increasing soil water content if soil temperature was high enough; when soil temperature was low, f_{bg}

368 was low despite the high soil water content as was the situation early in spring and late in autumn
369 (Fig. **7a**). When the dependency of f_{bg} on soil temperature and soil water content was analyzed
370 together, f_{bg} was positively correlated with soil temperature and soil water content in all seasons,
371 although most strongly in spring (Table **2c**). r^2 for the final model was 0.52.

372 f_{bg} of *A. glutinosa* decreased with increasing soil temperature (Table **2a**, Fig. **6b**), and increased with
373 increasing soil water content (Table **2b**, Fig. **7b**). f_{bg} seems to decrease with increasing soil
374 temperature because when soil temperature is high, soil water content is also typically low (Fig. **6b**).
375 This was verified by the fact that soil water content was the only significant variable to explain f_{bg}
376 when both soil temperature and water content were analyzed together (Table **2c**). In contrast, f_{bg} of *T.*
377 x *vulgaris* on a wet site increased with increasing soil temperature (Table **2a, c**, Fig. **6c**), and
378 decreased with increasing soil water content (Table **2b, c**, Fig. **6c**). The r^2 value (for the fixed effects)
379 in the final model was only 0.08 for *A. glutinosa* and 0.28 for *T.* x *vulgaris*. Based on the confidence
380 intervals of the model estimates, the effect of soil temperature on f_{bg} during summer was similar in *P.*
381 *sylvestris* and *T.* x *vulgaris* sites but significantly different in the *A. glutinosa* site, whereas the effect
382 of soil water content on f_{bg} during summer was similar in *P. sylvestris* and *A. glutinosa* sites and
383 significantly different in the *T.* x *vulgaris* site (when the effect of soil temperature and water content
384 were analyzed together, Table **2c**).

385 g_s was positively correlated with f_{bg} in all studied species (Table **3a**). The partial-corrected r^2 was 0.35
386 for *P. sylvestris*, 0.52 for *A. glutinosa* and 0.10 for *T.* x *vulgaris* (Table **3a**) indicating that
387 belowground hydraulic conductance explains 10 to 52% of the canopy conductance depending on the
388 case.

389 The modelled optimal canopy conductance predicted from eqn (1) was well correlated with the
390 measured canopy conductance in *P. sylvestris* with an r^2 of 0.78 (Table **3b**, Fig. **8**). When k_{bg} was
391 kept constant (and equal to k_{sl}) in the model, the correlation between the measured and modelled g_s

decreased significantly having r^2 of 0.46 (i.e. this is the explanatory power of the environmental factor C in eq. 8).

Discussion

The stomatal optimization model of Hölttä et al (2017) and Dewar et al (2018) provides a theoretical framework for the two key goals of our study: to examine the dependence of belowground hydraulic conductance (k_{bg}) on soil environment, and to examine the dependence of canopy conductance (g_s) on k_{bg}. In contrast to previous stomatal models which have various undetermined parameters – e.g. the parameter λ ("the cost of water") in the optimization theory of Cowan and Farquhar (1977) and Hari et al (1986), or the parameter g_1 in the empirical stomatal model of Ball et al (1987) and Medlyn et al (2013) – the present model contains no undetermined parameters. As a result, it makes the novel and specific prediction that soil environmental factors affect stomatal conductance (g_s) principally through their effect on below-ground hydraulic conductance (k_{bg}). Testing the validity of this prediction is important to our understanding of stomatal conductance because, if valid, it would enable the behaviour of tree gas exchange from contrasting sites to be understood and synthesised through an understanding of site-specific controls on k_{bg}.

Our results demonstrate that for mature *P. sylvestris* trees growing in field conditions, measured canopy conductance can indeed be successfully predicted from this optimization hypothesis, which explicitly relates g_s to soil-to-leaf hydraulic conductance, of which k_{bg} is an important component. Furthermore, we found that canopy conductance and k_{bg} were positively correlated in all studied species and sites (Table **3**). Our finding that canopy conductance is an increasing function of belowground hydraulic conductance, with a sensitivity that depends on environmental conditions, is consistent with the theoretical predictions summarized in eqns (8) and (9). In particular, the fit

between measured and modelled g_s was much better when measured k_{bg} was used to model g_s (r^2 = 0.78, Fig. **8**) than when k_{bg} was held constant in modelling g_s (r^2 = 0.46). The strong correlation between stomatal and plant conductance in their response to changes in environmental conditions makes sense from an evolutionary standpoint, from which one would expect selection for a coordinated response of stomata and plant tissues (Brodribb, Holbrook, Edwards & Gutiérrez, 2003; Sperry, 2000) to constrain the decrease in water potential with decreasing hydraulic conductance.

In conjunction with a strong positive correlation between k_{bg} and g_s, k_{bg} varied with soil temperature and soil water content in all tree species and sites studied here. Responses to soil drought mediated by leaf water potential have been shown to explain on average 87% of the observed decline in g_s in *Prunus dulcis, Olea europaea* and *Vitis vinifera* (Rodriguez-Dominguez et al, 2016). Also, elevated root-zone temperature has been shown to result in higher daytime stomatal conductance, transpiration and net assimilation rates in *Vitis vinifera* (Rogiers & Clarke, 2013). Soil temperature was the dominant factor controlling k_{bg} in *P. sylvestris* at the forest site: when soil temperature was low, k_{bg} was always low, but k_{bg} was often high even if soil water content was relatively low (Fig. **5**). The effect of soil water content on k_{bg} was overruled by soil temperature in spring and autumn. Especially in spring, the correlation between soil water content and k_{bg} was negative unless the effect of soil temperature was taken into consideration in the analysis. This is because soil water content and soil temperature had a negative correlation during spring and autumn. Soil temperature was over +8 °C during summer (according to our definition of seasons based on soil temperature), and thus the positive effect of soil water content on k_{bg} was most clear during summer. In summary, soil temperature was the limiting factor for the k_{bg} of *P. sylvestris* growing at a boreal forest site in spring and autumn, and soil water content in summer in the absence of low temperatures.

Environmental conditions for the urban street trees are more extreme than those in a forest stand. For example, air temperature is commonly higher, relative air humidity lower (i.e. D substantially higher),

439 and soil water and nutrient availability more limited in urban areas than in forests (Nielsen, Bühler &
440 Kristoffersen, 2007). This was evident in the high soil temperatures and large differences in soil water
441 content between individuals in the urban sites of this study. Soil water content was high throughout
442 the growing season for *T. x vulgaris* at the urban site, even excessively high, as further increase in
443 soil water content caused k_{bg} to decrease. A similar response in shoot growth was reported previously
444 for the same site and was explained by high groundwater level implying poor soil oxygen availability
445 (Riikonen, Lindén, Pulkkinen & Nikinmaa, 2011). k_{bg} of *A. glutinosa* growing at the urban site did
446 benefit from higher soil water content similarly to *P. sylvestris* at the forest site, most likely because
447 soil water content decreased clearly during summer months in both of these cases (Figs. **3**,**4**)
448 indicating that lack of water restricted hydraulic conductance periodically. Similarly, shoot growth
449 has been reported to respond positively to increase in soil water content at the *A. glutinosa* site
450 (Riikonen et al, 2011). Differences in the absolute values in soil water content between the forest site
451 and urban trees, and even between the urban trees, were mainly caused by different soil materials and
452 effectiveness of local drainage at the urban sites (Riikonen et al, 2011). Soil temperature did not have
453 a positive effect on k_{bg} at the *T. x vulgaris* site, unlike the other two studied cases, indicating that soil
454 temperature did not limit hydraulic conductance at the *T. x vulgaris* site during summer. This is
455 partially explained by the fact that the data from the broadleaved species growing in the urban sites
456 lacks the periods with cold soil temperatures in the leafless spring and autumn periods. The selected
457 tree species and site combinations form case studies to test the selected k_{bg} approach, and the study
458 design does not allow us to compare differences between species or sites per se; because both species
459 and sites vary between the studied cases, it is not possible to differentiate their effects individually.

460 The studied sites are located in boreal environment that can be characterized as cold and moist.
461 Temperature frequently drops to low values especially in spring and autumn, but soil water content
462 and soil water potential never drop to low values in spring, and rarely even in summer. The limiting
463 factors for k_{bg} are most likely different in drier and warmer environments. Using a similar

464 measurement approach as used in this study, the effect of soil water content on belowground hydraulic
465 conductance of *P. sylvestris* was recently studied in a dry Mediterranean forest (Poyatos et al, 2018).
466 Those results suggest that k_{bg} can become a limiting factor for whole-plant hydraulic conductance
467 during drought due to root embolism or reductions in the hydraulic conductance of the soil-root
468 interface (Poyatos et al, 2018). Martínez-Vilalta et al (2007), on the other hand, did not find a clear
469 relationship between k_{bg} and either soil temperature or soil water content in their study although the
470 method was similar. Their data was collected in Scotland from August to November. The climate in
471 Scotland is temperate and oceanic, and the measurement period represents late summer and autumn,
472 and thus it is possible that the scales of change in soil temperature and soil water content were not
473 large enough to effect k_{bg} in their study.

474 The method used to derive k_{bg} and g_s is based on continuous and automatic field measurements, which
475 is advantageous in comparison to measuring canopy gas exchange and soil and tree water potentials
476 directly. Earlier studies using different methodology have shown that k_{bg} decreases with decreasing
477 soil water content due to decreased soil hydraulic conductance (e.g. Campbell & Norman, 2000;
478 Duursma et al, 2008). In addition to soil water content, soil temperature has also been found to play
479 a key role in k_{bg} especially at low soil temperatures (BassiriRad et al, 1991; Cochard et al, 2000;
480 García-Tejera, López-Bernal, Villalobos, Orgaz & Testi, 2016; Mellander et al, 2004; Nobel et al,
481 1990; Running & Reid, 1980; Wan et al, 1999, 2001). However, studies of the relation between k_{bg}
482 and soil temperature have been missing in mature trees in field conditions. We found a steeper
483 decrease of k_{bg} with decreasing soil temperature in spring, when soil temperature was below +8°C
484 (Figs. **3**, **4, 5**); k_{bg} decreased below 0.3 of its maximum value mainly in spring and autumn. Also
485 Running and Reid (1980) found root resistance for water transport in *Pinus contorta* seedlings to
486 increase exponentially below +7 °C soil temperature, and Mellander et al (2004) found that soil
487 temperatures below +8 °C restricted transpiration, because of restricted water uptake in *P. sylvestris*.
488 The increase in belowground hydraulic conductance with increasing temperature is likely due to

489 decreasing water viscosity and increasing root membrane permeability due to modifications in its
490 fluidity (Améglio et al, 1990; Hertel & Steudle, 1997; Kaufmann, 1975; Kramer, 1940; Wan et al,
491 2001). For example, Wan et al (1999) showed with *Populus tremuloides* seedlings that root water
492 flow was decreased by decreasing soil temperature from 20 °C downwards. Decrease in water uptake
493 capacity with decreasing temperature cannot be fully explained by increasing water viscosity, but
494 requires also some other factors such as changes in root membrane permeability (Wan et al, 2001).
495 Consistent with this finding, Cochard et al. (2000) showed with *Quercus robur* saplings that
496 decreasing soil temperature decreased root conductance considerably, and that this decrease could be
497 explained by changes in water viscosity only in temperatures between 35 and 15 °C. The decrease in
498 root conductance was steeper in colder temperatures. Increase in root membrane permeability with
499 increasing temperature can be caused by biomembrane changes from a solid-gel state to a liquid-
500 crystal state (Améglio et al, 1990; Grossnickle, 1988) and/or by increased aquaporin activity (e.g.
501 Ionenko, Anisimov & Dautova, 2010; Javot & Maurel, 2002; Murai-Hatano et al, 2008). Moreover,
502 the growth of fine roots (Beikircher, Mittmann & Mayr, 2016; Larcher, 2003) and mycorrhizas
503 (Domisch, Finér, Lehto & Smolander, 2002) as well as restoration of the xylem hydraulic
504 conductivity after winter embolism (Beikircher et al, 2016) are strongly enhanced by increasing
505 temperatures, and thus increasing k_{bg}.

506 The method of estimating belowground hydraulic conductance from simultaneous field
507 measurements of sap flow rate and xylem diameter change of mature trees gave consistent values
508 over the seasonal time series of k_{bg} across years, tree individuals, species and sites, and of the variation
509 of k_{bg} with soil temperature, soil water content, and canopy conductance. Our results demonstrate that
510 soil temperature is an important factor affecting the water availability and the leaf gas exchange of
511 mature trees in boreal conditions. The expected earlier snowmelt and higher springtime soil
512 temperatures (Mellander, Löfvenius & Laudon, 2007) are expected to accelerate springtime carbon
513 uptake (Black et al, 2000; Pulliainen et al, 2017) and allow the growing season to start earlier (Bergh

& Linder, 1999), leading to increased carbon sequestration and growth in boreal conditions (Jarvis & Linder, 2000). Our results indicate how such effects may be represented in models, through the use of a novel stomatal optimization theory that links stomatal conductance to belowground hydraulic conductance.

Author Contribution

TH and AL conceived the study. The measurements were maintained and data quality checked at SMEAR II by TP and at the urban site by AR. Data was pre-processed by TP and analyzed by AL. YS participated in the discussions on data analysis. Stomatal model formulations for comparing the measured and modelled stomatal conductance were written by RD. AL had the main responsibility for writing the manuscript, but all authors contributed to the writing.

527 **References**

528 Aalto J., Porcar-Castell A., Atherton J., Kolari P., Pohja T., Hari P., Nikinmaa E., Petäjä T. & Bäck
529 J. (2015). Onset of photosynthesis in spring speeds up monoterpene synthesis and leads to emission
530 bursts. *Plant Cell Environ.*, 38, 2299-2312.

531 Aalto J., Scherrer D., Lenoir J., Guisan A. & Luoto M. (2018). Biogeophysical controls on soil-
532 atmosphere thermal differences: implications on warming Arctic ecosystems. *Environ. Res. Lett.*,
533 13, 074003.

534 Alméras T. (2008). Mechanical analysis of the strains generated by water tension in plant stems.
535 Part II: strains in wood and bark and apparent compliance. *Tree Physiol.*, 28, 1513-1523.

536 Alméras T. & Gril J. (2007). Mechanical analysis of the strains generated by water tension in plant
537 stems. Part I: stress transmission from the water to the cell walls. *Tree Physiol.*, 27, 1505-1516.

538 Améglio T., Morizet J., Cruiziat P., Martignac M., Bodet C. & Raynaud H. (1990). The effects of
539 root temperature on water flux, potential and root resistance in sunflower. *Agronomie*, 10, 331-340.

540 Badal E., Buesa I., Guerra D., Bonet L., Ferrer B. & Intrigliolo D.S. (2010). Maximum diurnal
541 trunk shrinkage is a sensitive indicator of plant water stress in *Diospyros kaki* (Persimmon) trees.
542 *Agr. Water Manage.*, 98, 143-147.

543 Ball J.T., Woodrow I.E. & Berry J.A. (1987). A model predicting stomatal conductance and its
544 contribution to the control of photosynthesis under different environmental conditions. In: Biggins
545 J, ed. *Progress in Photosynthesis Research*. Martinus-Nijhoff Publishers, Dordrecht, The
546 Netherlands, 221-224.

547 BassiriRad H., Radin J.W. & Matsuda, K. (1991). Temperature-dependent water and ion transport
548 properties of barley and sorghum roots I. Relationship to leaf growth. *Plant Physiol.*, 97, 426-432.

549 Beikircher B., Mittmann C. & Mayr S. (2016). Prolonged soil frost affects hydraulics and
550 phenology of apple trees. *Front. Plant Sci.*, 7, 867.

551 Bergh J. & Linder S. (1999). Effects of soil warming during spring on photosynthetic recovery in
552 boreal Norway spruce stands. *Glob. Change Biol.*, 5, 245-253.

553 Black T.A., Chen W.J., Barr A.G., Arain M.A., Chen Z., Nesic Z, Hogg E.H., Neumann H.H. &
554 Yang P.C. (2000). Increased carbon sequestration by a boreal deciduous forest in years with a warm
555 spring. *Geophys. Res. Letters*, 27, 1271-1274.

556 Böttcher K., Markkanen T., Thum T., Aalto T., Aurela M., Reick C.H., Kolari P., Arslan A.N. &
557 Pulliainen J. (2016). Evaluating biosphere model estimates of the start of the vegetation active
558 season in Boreal forests by satellite observations. *Remote Sens.*, 8, 580.

559 Bréda N., Granier A., Barataud F. & Moyne J. (1995). Soil water dynamics in an oak stand I. Soil
560 moisture, water potentials and water uptake by roots. *Plant Soil*, 172, 17-27.

561 Brodribb T.J., Holbrook N.M., Edwards E.J. & Gutiérrez M.V. (2003). Relations between stomatal
562 closure, leaf turgor and xylem vulnerability in eight tropical dry forest trees. *Plant Cell Environ.*, 26,
563 443-450.

564 Cajander A.K. (1949). Forest types and their significance. *Acta For. Fenn*., 56, 1-69.

565 Campbell G.S. & Norman J.M. (2000). *Introduction to environmental biophysics*. New York, NY,
566 USA: Springer-Verlag.

567 Ĉermák J., Huzulák J. & Penka M. (1980). Water potential and sap flow rate in adult trees with
568 moist and dry soil as used for the assessment of root system depth. *Biol. plantarum*, 22, 34-41.

569 Cochard C., Martin R., Gross P. & Bogeat-Triboulot M.B. (2000). Temperature effects on hydraulic
570 conductance and water relations of *Quercus robur* L. *J. Exp. Bot.*, 51, 1255-1259.

571 Cochard H., Forestier S. & Améglio T. (2002). A new validation of the Scholander pressure
572 chamber technique based on stem diameter variations. *J. Exp. Bot.*, 52, 1361-1365.

573 Comstock J. & Mencuccini M. (1998). Control of stomatal conductance by leaf water potential in
574 *Hymenoclea salsola* (T. & G.), a desert subshrub. *Plant Cell Environ.*, 21, 1029-1038.

575 Cowan I.R. & Farquhar G.D. (1977). Stomatal function in relation to leaf metabolism and
576 environment. In: Jennings DH, ed. *Integration of Activity in the Higher Plant*. Cambridge
577 University Press, Cambridge, 471-505.

578 Day T.A., Heckathorn S.A. & DeLucia E.H. (1991). Limitations of photosynthesis in *Pinus taeda*
579 L. (loblolly pine) at low soil temperatures. *Plant Physiol*., 96, 1246-1254.

580 Delucia E.H. (1986). Effect of low root temperature on net photosynthesis, stomatal conductance
581 and carbohydrate concentration in Engelmann spruce (*Picea engelmannii* Parry ex Engelm.)
582 seedlings. *Tree Physiol.*, 2, 143-154.

583 Dewar R., Mauranen A., Mäkelä A., Hölttä T., Medlyn B. & Vesala T. (2018). New insights into
584 the covariation of stomatal, mesophyll and hydraulic conductances from optimization models
585 incorporating nonstomatal limitations to photosynthesis. *New Phytol.*, 217, 571-585.

586 Dietrich L., Zweifel R. & Kahmen A. (2018). Daily stem diameter variations can predict the canopy
587 water status of mature temperate trees. *Tree Physiol*., 38, 941-952.

588 Domisch T., Finér L., Lehto T. & Smolander A. (2002). Effect of soil temperature on nutrient
589 allocation and mycorrhizas in Scots pine seedlings. *Plant Soil*, 239, 173-185.

590 Donovan L.A., Linton M.J. & Richards J.H. (2001). Predawn plant water potential does not
591 necessarily equilibrate with soil water potential under well-watered conditions. *Oecologia*, 129,
592 328-335.

593 Duursma R.A., Kolari P., Perämäki M., Nikinmaa E., Hari P., Delzon S., Loustau D., Ilvesniemi H.,
594 Pumpanen J. & Mäkelä A. (2008). Predicting the decline in daily maximum transpiration rate of
595 two pine stands during drought based on constant minimum leaf water potential and plant hydraulic
596 conductance. *Tree Physiol.*, 28, 265-276.

597 Fahey T.J. & Young D.R. (1984). Soil and xylem water potential and soil water content in
598 contrasting *Pinus contorta* ecosystems, Southeastern Wyoming, USA. *Oecologia*, 61, 346-351.

599 Friend A.D. (1991). Use of a model of photosynthesis and leaf microenvironment to predict optimal
600 stomatal conductance and leaf nitrogen partitioning. *Plant Cell Environ.*, 14, 895-905

601 García-Tejera O., López-Bernal A., Villalobos F.J., Orgaz F. & Testi L. (2016). Effect of soil
602 temperature on root resistance: implications for different trees under Mediterranean conditions. *Tree*
603 *Physiol.*, 36, 469-478.

604 Garnier E. & Berger A. (1987). The influence of drought on stomatal conductance and water
605 potential of peach trees growing in the field. *Sci. Hortic.*, 32, 249-263.

606 Gimeno T.E., Saavedra N., Ogée J., Medlyn B.E. & Wingate L. (2019). A novel optimization
607 approach incorporating non-stomatal limitations predicts stomatal behaviour in species from six
608 plant functional types. *J. Exp. Bot.*, 70, 1639-1651.

609 Givnish T.I. (1986). Optimal stomatal conductance. Allocation of energy between leaves and roots,
610 and the marginal cost of transpiration. In: Givnish TI, ed. *On the Economy of Plant Form and*
611 *Function.* Cambridge University Press, Cambridge, 171-213.

612 Granier A. (1987). Evaluation of transpiration in a Douglas-fir stand by means of sap flow
613 measurements. *Tree Physiol.*, 3, 309-320.

614 Grossnickle S.C. (1988). Planting stress in newly planted jack pine and white spruce. 1 Factors
615 influencing water uptake. *Tree Physiol.*, 4, 71-83.

616 Hari P., Mäkelä A., Korpilahti E. & Holmberg M. (1986). Optimal control of gas exchange. *Tree*
617 *Physiol*., 2, 169-175.

618 Hari P. & Kulmala M. (2005). Station for Measuring Ecosystem–Atmosphere Relations (SMEAR
619 II). *Boreal Environ. Res.*, 10, 315-322.

620 Hertel A. & Steudle E. (1997). The function of water channels in Chara: the temperature
621 dependence of water and solute flows provides evidence for composite membrane transport and for
622 a slippage of small organic solutes across water channels. *Planta*, 202, 324-335.

623 Hölttä T., Linkosalo T., Riikonen A., Sevanto S. & Nikinmaa E. (2015). An analysis of Granier sap
624 flow method, its sensitivity to heat storage and a new approach to improve its time dynamics. *Agr.*
625 *Forest Meteorol.*, 211, 2-12.

626 Hölttä T., Lintunen A., Chan T., Mäkelä A. & Nikinmaa E. (2017). A steady-state stomatal model
627 of balanced leaf gas exchange, hydraulics and maximal source–sink flux. *Tree Physiol.*, 37, 851-
628 868.

629 Hölttä T., Vesala T., Nikinmaa E., Perämäki M., Siivola E. & Mencuccini M. (2005). Field
630 measurements of ultrasonic acoustic emissions and stem diameter variations. New insight into the
631 relationship between xylem tensions and embolism. *Tree Physiol.*, 25, 237-243.

632 Irvine J. & Grace J. (1997). Continuous measurements of water tensions in the xylem of trees based
633 on the elastic properties of wood. *Planta*, 202, 455-461.

634 Intrigliolo D.S., Puerto H., Bonet L., Alarcón J.J., Nicolas E. & Bartual J. (2011). Usefulness of
635 trunk diameter variations as continuous water stress indicators of pomegranate (*Punica granatum*)
636 trees. *Agr. Water Manage.*, 98, 1462-1468.

637 Ionenko I.F., Anisimov A.V. & Dautova N.R. (2010). Effect of temperature on water transport
638 through aquaporins. *Biol. Plantarum*, 54, 488-494.

639 IPCC 2018. Global warming of 1.5°C. An IPCC Special Report on the impacts of global
640 warming of 1.5°C above pre-industrial levels and related global greenhouse gas emission
641 pathways, in the context of strengthening the global response to the threat of climate change,
642 sustainable development, and efforts to eradicate poverty [V. Masson-Delmotte, P. Zhai, H. O.
643 Pörtner, D. Roberts, J. Skea, P.R. Shukla, A. Pirani, W. Moufouma-Okia, C. Péan, R. Pidcock, S.
644 Connors, J. B. R. Matthews, Y. Chen, X. Zhou, M. I. Gomis, E. Lonnoy, T. Maycock, M. Tignor, T.
645 Waterfield (eds.)].

646 Järvi L., Hannuniemi H., Hussein T., Junninen H., Aalto P.P., Hillamo R., Mäkelä T., Keronen P.,
647 Siivola E., Vesala T. & Kulmala M. (2009). The urban measurement station. SMEAR III:
648 continuous monitoring of air pollution and surface-atmosphere interactions in Helsinki, Finland.
649 *Boreal Environ. Res.* 14 (Suppl A): 86-109.

650 Jarvis P. & Linder S. (2000). Constraints to growth of boreal forests. *Nature*, 405, 904-905.

651 Javot H. & Maurel C. (2002). The role of aquaporins in root water uptake. *Ann Bot.*, 90, 301-303.

652 Kaufmann M.R. (1975). Leaf water stress in Engelmann spruce: influence of the root and shoot
653 environments. *Plant Physiol*., 56, 841-844.

654 Kolari P., Lappalainen H.K., Hänninen H. & Hari P. (2007). Relationship between temperature and
655 the seasonal course of photosynthesis in Scots pine at northern timberline and in southern boreal
656 zone. *Tellus*, 59B, 542-552.

657 Kramer P.J. (1940). Root resistance as a cause of decreased water adsorption by plants at low
658 temperatures. *Plant Physiol.*, 15, 63-79.

659 Larcher W. (2003). *Physiological Plant Ecology*. Berlin: Springer Verlag.

660 Lindfors L., Hölttä T., Lintunen A., Porcar-Castell A., Nikinmaa E. & Juurola E. (2015). Dynamics
661 of leaf gas exchange, chlorophyll fluorescence and stem diameter changes during freezing and
662 thawing of Scots pine seedlings. *Tree Physiol.*, 35, 1314-1324.

663 Lintunen A., Paljakka T., Salmon Y. & Hölttä T. (2018). Belowground hydraulic conductance in a
664 mature boreal Scots pine tree. *Acta Hortic.*, 1222, 103-108.

665 Lintunen A., Paljakka T., Riikonen A., Lindén L., Lindfors L., Nikinmaa E. & Hölttä T. (2015).
666 Irreversible diameter change of branches correlates with other methods for estimating frost
667 tolerance of living cells in freeze- thaw experiment: a case study with seven urban tree species in
668 Helsinki. *Ann. For. Sci.*, 72, 1089-1098.

669 Lippu J. & Puttonen P. (1991). Soil temperature limitations on gas exchange in 1-year-old *Pinus*
670 *sylvestris* (L) seedlings. *Scand. J. For. Res.*, 6, 73-78.

671 Lu P., Urban L. & Zhao P. (2004). Granier's thermal dissipation probe (TDP) method for measuring
672 sap flow in trees: theory and practice. *Acta Bot. Sin.*, 46, 631-646.

673 Martínez-Vilalta J., Cochard H., Mencuccini M., Sterck F., Herrero A., Korhonen J. F. J., Llorens
674 P., Nikinmaa E., Nolè A., Poyatos R., Ripullone F., Sass-Klaassen U. & Zweifel R. (2009).
675 Hydraulic adjustment of Scots pine across Europe. *New Phytol.*, 184, 353-364.

676 Martínez-Vilalta J., Korakaki E., Vanderklein D. & Mencuccini M. (2007). Below-ground hydraulic
677 conductance is a function of environmental conditions and tree size in Scots pine. *Funct. Ecol.*, 21,
678 1072-1083.

679 McElrone A.J., Bichler J., Pockman W.T., Addington R.N., Linder C.R. & Jackson R.B. (2007).
680 Aquaporin-mediated changes in hydraulic conductivity of deep tree roots accessed via caves. *Plant*
681 *Cell Environ.*, 30, 1411-1421.

682 McLean E.H., Ludwig M. & Grierson P.F. (2011). Root hydraulic conductance and aquaporin
683 abundance respond rapidly to partial root-zone drying events in a riparian *Melaleuca* species. *New*
684 *Phytol.*, 192, 664-675.

685 Medlyn B.E., Duursma R., De Kauwe M.G. & Prentice I.C. (2013). The optimal stomatal response
686 to atmospheric CO_2: Alternative solutions, alternative interpretations. *Agr. Forest Meteorol.*, 182-
687 183, 200-203.

688 Mellander P.-E., Bishop K. & Lundmark T. (2004). The influence of soil temperature on
689 transpiration: a plot scale manipulation in a young Scots pine stand. *Forest Ecol. Manage.*, 195, 15-
690 28.

691 Mellander P.-E., Löfvenius M.O. & Laudon H. (2007). Climate change impact on snow and soil
692 temperature in boreal Scots pine stands. *Climatic Change*, 85, 179-193.

693 Meng Z., Duan A., Chen D., Bandara Dassanayake K., Wang X., Liu Z., Liu H. & Gao S. (2017).
694 Suitable indicators using stem diameter variation-derived indices to monitor the water status of
695 greenhouse tomato plants. *PLOS ONE*: DOI:10.1371/journal.pone.0171423

696 Murai-Hatano M., Kuwagata T., Sakurai J., Nonami H., Ahamed A., Nagasuga K., Matsunami T.,
697 Fukushi K., Maeshima M. & Okada M. (2008). Effect of low root temperature on hydraulic
698 conductivity of rice plants and the possible role of aquaporins. *Plant Cell Physiol.*, 49, 1294-1305.

699 Nielsen C.N., Bühler O. & Kristoffersen P. (2007). Soil water dynamics and growth of street and
700 park trees. *Arboriculture Urban Forest.*, 33, 231-245.

701 Niittynen P., Heikkinen R.K. & Luoto M. (2018). Snow cover is a neglected driver of Arctic
702 biodiversity loss. *Nat. Clim. Change*, 8, 997-1001.

703 Nobel P.S. (2009) Physicochemical and environmental plant physiology. Academic Press, San
704 Diego.

705 Nobel P.S., Schulte P.J. & North G.B. (1990). Water influx characteristics and hydraulic
706 conductivity for roots of *Agave deserti* Engelm. *J. Exp. Bot.*, 41, 409-415.

707 Offenthaler I., Hietz P. & Richter H. (2001). Wood diameter indicates diurnal and long-term
708 patterns of xylem water potential in Norway spruce. *Trees*, 15, 215-221.

709 Ortuño M.F., García-Orellana Y., Conejero W., Ruiz-Sánchez M.C., Mounzer O., Alarcón J.J. &
710 Torrecillas A. (2006). Relationships between climatic variables and sap flow, stem water potential
711 and maximum daily trunk shrinkage in lemon trees. *Plant Soil*, 279, 229-242.

712 Perämäki M., Nikinmaa E., Sevanto S., Ilvesniemi H., Siivola E., Hari P. & Vesala T. (2001). Tree
713 stem diameter variations and transpiration in Scots pine: an analysis using a dynamic sap flow
714 model. *Tree Physiol.*, 21, 889-897.

715 Poyatos, R., Aguadé, D., Martínez-Vilalta, J. (2018). Below-ground hydraulic constraints during
716 drought-induced decline in Scots pine. *Ann. For. Sci.*, 75, 100 https://doi.org/10.1007/s13595-018-
717 0778-7

718 Pulliainen J., Aurela M., Laurila T., Aalto T., Takala M., Salminen M., Kulmala M., Barr A.,
719 Heimann M., Lindroth A., Laaksonen A., Derksen C., Mäkelä A., Markkanen T., Lemmetyinen J.,
720 Susiluoto J., Dengel S., Mammarella I., Tuovinen J.-P. & Vesala T. (2017). Early snowmelt
721 significantly enhances boreal springtime carbon uptake. *PNAS*, 114, 11081-11086.

722 Riikonen A., Järvi L. & Nikinmaa E. (2016). Environmental and crown related factors affecting
723 street tree transpiration in Helsinki, Finland. *Urban Ecosyst.*, 19, 1693-1715.

724 Riikonen A., Lindén L., Pulkkinen M. & Nikinmaa E. (2011). Post-transplant crown allometry and
725 shoot growth of two species of street trees. *Urban For. Urban Gree.*, 10, 87-94.

726 Rissanen K., Hölttä T., Vanhatalo A., Aalto J., Nikinmaa E., Rita H. & Bäck J. (2016). Diurnal
727 patterns in Scots pine stem oleoresin pressure in a boreal forest. *Plant Cell Environ.*, 39, 527-538.

728 Rodriguez-Dominguez C.M., Buckley T.N., Egea G., de Cires A., Hernandez-Santana V., Martorell
729 S. & Diaz-Espejo A. (2016). Most stomatal closure in woody species under moderate drought can
730 be explained by stomatal responses to leaf turgor. *Plant Cell Environ.*, 39, 2014-2026.

731 Rogiers S.Y. & Clarke S.J. (2013). Nocturnal and daytime stomatal conductance respond to root-
732 zone temperature in 'Shiraz' grapevines. *Ann. Bot.*, 111, 433-444.

733 Rosner S., Karlsson B., Konnerth J. & Hansmann C. (2009). Shrinkage processes in standard-size
734 Norway spruce wood specimens with different vulnerability to cavitation. *Tree Physiol.*, 29, 1419-
735 1431.

736 Rosner S., Konnerth J., Plank B., Salaberger D. & Hansmann C. (2010). Radial shrinkage and
737 ultrasound acoustic emissions of fresh versus pre-dried Norway spruce sapwood. *Trees*, 24, 931-
738 940.

739 Running S.W. & Reid C.P. (1980). Soil temperature influences on root resistance of *Pinus contorta*
740 seedlings. *Plant Physiol.*, 65, 635-640.

741 Sala O.E., Lauenroth W.K., Parton W.J. & Trlica M.J. (1981). Water status of soil and vegetation in
742 a shortgrass steppe. *Oecologia,* 48, 327-331.

743 de Santana M.J., de Almeida Bocate G., Sgobi M.A., Borges Valeriano T.T. & de Souza S.S.
744 (2017). Irrigation management of muskmelon with tensiometry. *Revista Agrogeoambiental*, 9, 71-
745 79.

746 Sevanto S., Hölttä T., Hirsikko A., Vesala T. & Nikinmaa E. (2005a). Determination of thermal
747 expansion of green wood and the accuracy of tree stem diameter variation measurements. *Boreal*
748 *Environ. Res.*, 10: 437-445.

749 Sevanto S., Hölttä T., Markkanen T., Perämäki M., Nikinmaa E. & Vesala T. (2005b).
750 Relationships between diurnal xylem diameter variation and environmental factors in Scots pine.
751 *Boreal Environ. Res.*, 10, 447-458.

752 Shipley B. (2016). *Cause and Correlation in Biology: A User's Guide to Path Analysis, Structural*
753 *Equations and Causal Inference with R*. Cambridge University Press.

754 Sperry J.S. (2000). Hydraulic constraints on plant gas exchange. *Agr. Forest Meteorol.*, 104, 13-23.

755 Ueda M. & Shibata E. (2001). Diurnal changes in branch diameter as indicator of water status of
756 Hinoki cypress *Chamaecyparis obtuse*. *Trees,* 15, 315-318.

757 Wan X., Landhäusser S.M., Zwiazek J.J. & Lieffers V.J. (1999). Root water flow and growth of
758 aspen (*Populus tremuloides*) at low root temperatures. *Tree Physiol.*, 19, 879-884.

759 Wan X., Zwiazek J.J., Lieffers V.J. & Landhäusser S.M. (2001). Hydraulic conductance in aspen
760 (*Populus tremuloides*) seedlings exposed to low root temperatures. *Tree Physiol.*, 20, 691-696.

761

762 **Supporting Information** includes derivation of optimal stomatal conductance and its dependence
763 on belowground hydraulic conductance (main text equations 1 and 8).

Tables

Table 1. List of symbol definitions and units used in the main text.

Symbol	Definition	Unit
A	leaf photosynthesis	mol m^{-2} s^{-1}
A_{leaf}	leaf area	m^2
α_0	photosynthetic quantum yield	mol mol^{-1}
c_a	atmospheric CO_2 concentration	mol mol^{-1}
c_i	intercellular CO_2 concentration	mol mol^{-1}
D	vapor pressure deficit	mol mol^{-1}
D_{max}	maximum daily vapor pressure deficit	mol mol^{-1}
dx_{max}	daily maximum xylem diameter (mean of the 10 % highest values)	µm
dx_{min}	daily minimum xylem diameter (mean of the 10 % lowest values)	µm
Δdx	daily amplitude of diameter change	µm
f_{bg}	normalized belowground hydraulic conductance (values 0-1)	-
F_{max}	daily maximum sap flow rate (mean of the 10 % highest values)	l h^{-1}
g_s	canopy conductance for CO_2	mol m^{-2} s^{-1}
$g_{s,norm}$	normalized canopy conductance (values 0-1)	-
k_{bg}	belowground hydraulic conductance	mol m^{-2} s^{-1} MPa^{-1}
$k_{bg,d}$	daily maximum belowground hydraulic conductance	mol m^{-2} s^{-1} MPa^{-1}
$k_{bg,max}$	annual maximum hydraulic conductance	mol m^{-2} s^{-1} MPa^{-1}
k_{rl}	leaf specific base-to-leaf hydraulic conductance	mol m^{-2} s^{-1} MPa^{-1}
k_{sl}	leaf specific soil-to-leaf hydraulic conductance	mol m^{-2} s^{-1} MPa^{-1}
ψ_c	critical leaf water potential	MPa
ψ_l	leaf water potential	MPa
ψ_s	soil water potential	MPa
Q	photosynthetically active radiation	mol m^{-2} s^{-1}
Γ^*	CO_2 photorespiratory compensation point	mol mol^{-1}
$r_{x,0}$	carboxylation resistance in the absence of non-stomatal limitation	mol^{-1} m^2 s
SWC	soil water content (relative value)	-

Table 2. Mixed effect model results are presented for normalized belowground hydraulic conductance (f_{bg}) for *Pinus sylvestris*, *Alnus glutinosa* and *Tilia x vulgaris*. A) f_{bg} is modelled with daily mean soil temperature (ST) as an independent variable, B) with soil water content (SWC) as an independent variable, and C) with a full model selected based on Akaike's Information Criteria. For *Pinus*, season and its interaction variable with ST and SWC are also included in all models. Seasons refer to spring (SP), autumn (AU) and summer (SU). r^2 is given for the fixed effects only.

Species	Dependent variable	r^2	Effect	Season	Estimate	Confidence interval (95)	Standard Error	t Value	Pr > |t|
A									
Pinus	f_{bg}	0.44	Intercept		0.46	0.26-0.67	0.065	7.17	0.0056
			season	SP	-0.40	-0.54-(-0.25)	0.074	-5.38	<.0001
			season	AU	-0.64	-1.02-(-0.26)	0.194	-3.31	0.0010
			season	SU	0	.	.	.	.
			ST		0.01	0.00-0.02	0.006	2.19	0.0288
			ST*season	SP	0.068	0.05-0.09	0.009	7.46	<.0001
			ST*season	AU	0.056	0.00-0.11	0.028	2.04	0.0415
			ST*season	SU	0	.	.	.	.
Alnus	f_{bg}	0.02	Intercept		0.54	0.25-0.83	0.067	8.11	0.0149
			ST		-0.01	-0.01-(0.00)	0.002	-3.85	0.0001
Tilia	f_{bg}	0.22	Intercept		0.05	-0.15-0.26	0.047	1.11	0.3821
			ST		0.02	0.02-0.03	0.002	10.54	<.0001
B									
Pinus	f_{bg}	0.32	Intercept		0.47	0.35-0.59	0.037	12.81	0.0010
			season	SP	0.51	0.27-0.75	0.121	4.22	<.0001
			season	AU	-0.17	-0.31-(0.04)	0.069	-2.51	0.0124
			season	SU	0	.	.	.	.
			SWC		0.66	0.34-0.98	0.164	4.01	<.0001
			SWC*seaso	SP	-2.31	-3.09-(-1.55)	0.391	-5.91	<.0001
			SWC*seaso	AU	-0.74	-1.42-(-0.05)	0.348	-2.12	0.0343
			SWC*seaso	SU	0	.	.	.	.
Alnus	f_{bg}	0.07	Intercept		0.15	-0.15-0.45	0.070	2.12	0.1683
			SWC		1.47	1.02-1.92	0.229	6.40	<.0001
Tilia	f_{bg}	0.18	Intercept		2.17	1.41-2.93	0.176	12.35	0.0065
			SWC		-8.10	-9.74-(-6.46)	0.835	-9.71	<.0001
C									
Pinus	f_{bg}	0.52	Intercept		0.13	-0.12-0.37	0.078	1.62	0.2028
			season	SP	-1.46	-1.87-(-1.05)	0.208	-6.99	<.0001
			season	AU	-0.46	-0.87-(-0.05)	0.209	-2.19	0.0291
			season	SU	0	.	.	.	.
			SWC		1.01	0.72-1.30	0.147	6.89	<.0001
			ST		0.02	0.01-0.04	0.005	4.54	<.0001
			ST*season	SP	0.11	0.09-0.13	0.012	9.67	<.0001
			ST*season	AU	0.05	0.00-0.11	0.026	2.07	0.0387
			ST*season	SU	0	.	.	.	.
			SWC*seaso	SP	2.45	1.47-3.43	0.499	4.92	<.0001
			SWC*seaso	AU	-0.58	-1.18-(0.02)	0.305	-1.90	0.0586
			SWC*seaso	SU	0	.	.	.	.
Alnus	f_{bg}	0.08	Intercept		0.11	-0.35-0.57	0.107	1.06	0.4011
			SWC		1.56	0.95-2.16	0.309	5.04	<.0001
			ST		0.00	-0.00-(0.01)	0.003	0.43	0.6703
Tilia	f_{bg}	0.28	Intercept		1.20	0.24-2.16	0.223	5.37	0.0330
			SWC		-4.89	-6.73-(-3.06)	0.934	-5.24	<.0001
			ST		0.02	0.01-0.02	0.003	6.52	<.0001

Table 3. A) Mixed effect model results are presented for the correlation between normalized (measured) canopy conductance (g_s) and belowground hydraulic conductance (f_{bg}) for *Pinus sylvestris*, *Alnus glutinosa* and *Tilia x vulgaris*. Season is included in the model selection process for *P. sylvestris*; seasons refer to spring (SP), autumn (AU) and summer (SU). The models are selected based on Akaike's Information Criteria. We used log-transformed values, because the data had a power-law form. B) Generalized linear model results are given for the relation between measured (unnormalized) and modelled canopy conductance (g_s) for *P. sylvestris*. r^2 is given for fixed effects only, and corrected r^2 is given in A as calculated in eq. 10.

Species	Dependent variable	r^2	Effect	Season	Estimate	Confidence interval (95)	Standard Error	t Value	Pr > |t|
A									
Pinus	g_{s_norm}	0.35	Intercept		-0.26	-0.48-(-0.03)	0.071	-3.61	0.0366
			season	SP	-0.04	-0.16-(0.09)	0.064	-0.60	0.5515
			season	AU	-0.46	-0.72-(-0.20)	0.132	-3.45	0.0006
			season	SU	0	.	.	.	.
			f_{bg}		0.76	0.63-0.89	0.066	11.52	<.0001
			f_{bg} *season	SP	0.10	-0.05-0.26	0.078	1.29	0.1972
			f_{bg} *season	AU	-0.24	-0.45-(-0.04)	0.106	-2.30	0.0220
			f_{bg} *season	SU	0	.	.	.	.
Alnus	g_{s_norm}	0.52	Intercept		-0.43	-0.87-0.02	0.104	-4.09	0.0550
			f_{bg}		0.91	0.83-0.99	0.042	21.71	<.0001
Tilia	g_{s_norm}	0.10	Intercept		-0.25	-0.86-0.36	0.143	-1.75	0.2216
			f_{bg}		0.92	0.86-0.97	0.028	32.92	<.0001
B									
Pinus	$g_{s\_measured}$	0.78	Intercept		-0.00	-0.01-0.01	0.002	-0.42	0.7131
			$g_{s\_modelled}$		1.02	0.96-1.08	0.031	33.21	<.0001

785 **Figure captions**

786 Figure 1. A) Relationship between xylem diameter and stem water potential in *Alnus glutinosa* grown
787 in an urban environment. The measurements are from morning, mid-day and afternoon for 5 days in
788 June in 2011. B) Relationship between maximum diurnal xylem diameter and soil water potential in
789 cases where soil water potential is essentially different from zero in *Pinus sylvestris* grown in a forest
790 stand. The measurements are from May to August in 2015. In both figures, xylem diameter is set to
791 zero in the beginning of the period.

792 Figure 2. Illustration of the principle used in deriving daily belowground hydraulic conductance (k_{bg})
793 and canopy conductance (g_s) from 24 hours of example field data. F_{max}, dx_{max} and D_{max} are calculated
794 as mean of the 10 % highest values per day and dx_{min} as mean of the 10% lowest values per day.

795 Figure 3. Time series of A) normalized belowground hydraulic conductance (f_{bg}), B) daily maximum
796 sap flow rate (F_{max}), C) the daily amplitude of diameter change (Δdx) and daily maximum vapor
797 pressure deficit (D_{max}), and D) daily mean soil temperature and soil water content for *Pinus sylvestris*
798 grown in a forest stand (tree 1 in year 2015).

799 Figure 4. Time series of A) normalized belowground hydraulic conductance (f_{bg}), B) daily maximum
800 sap flow rate (F_{max}), C) the daily amplitude of diameter change (Δdx) and daily maximum vapor
801 pressure deficit (D_{max}), and D) daily mean soil temperature and soil water content for *Alnus glutinosa*
802 grown in urban environment (tree 2 in year 2010). f_{bg} data are shown only for the leaf-period (period
803 between the leaf area reached 15% of its total area in spring and before the leaf fall had reached 70%
804 of its total area in autumn).

805 Figure 5. Time series of A) normalized belowground hydraulic conductance (f_{bg}), B) daily maximum
806 sap flow rate (F_{max}), C) the daily amplitude of diameter change (Δdx) and daily maximum vapor
807 pressure deficit (D_{max}), and D) daily mean soil temperature and soil water content for *Tilia x vulgaris*

808 grown in urban environment (tree 1 in year 2013). f_{bg} data are shown only for the leaf-period (period
809 between the leaf area reached 15% of its total area in spring and before the leaf fall had reached 70%
810 of its total area in autumn).

811 Figure 6. Normalized belowground hydraulic conductance (f_{bg}) plotted against daily mean soil
812 temperature in spring, summer and autumn for A) *Pinus sylvestris* trees grown in a forest stand, B)
813 *Alnus glutinosa* grown in an urban environment, and C) *Tilia x vulgaris* grown in an urban
814 environment. The bubble size represents volumetric soil water content. Linear fits between f_{bg} and
815 soil temperature are drawn and r^2 values are given for each season in A and for all data in B and C.
816 See Table 2A for detailed analysis. Note different X-axes values in the panels.

817 Figure 7. Normalized belowground hydraulic conductance (f_{bg}) plotted against volumetric soil water
818 content in spring, summer and autumn for A) *Pinus sylvestris* trees grown in a forest stand, B) *Alnus*
819 *glutinosa* grown in an urban environment, and C) *Tilia x vulgaris* grown in an urban environment.
820 The bubble size represents relative soil temperature. Linear fits between f_{bg} and soil temperature are
821 drawn and r^2 values are given for each season in A and for all data in B and C. See Table 2B for
822 detailed analysis. Note different X-axes values in the panels.

823 Figure 8. Measured canopy conductance (g_s) for *Pinus sylvestris* compared with canopy conductance
824 modelled using eqns 8 and 9. See Table 3 for detailed analysis.

825

826

827

828

Figures

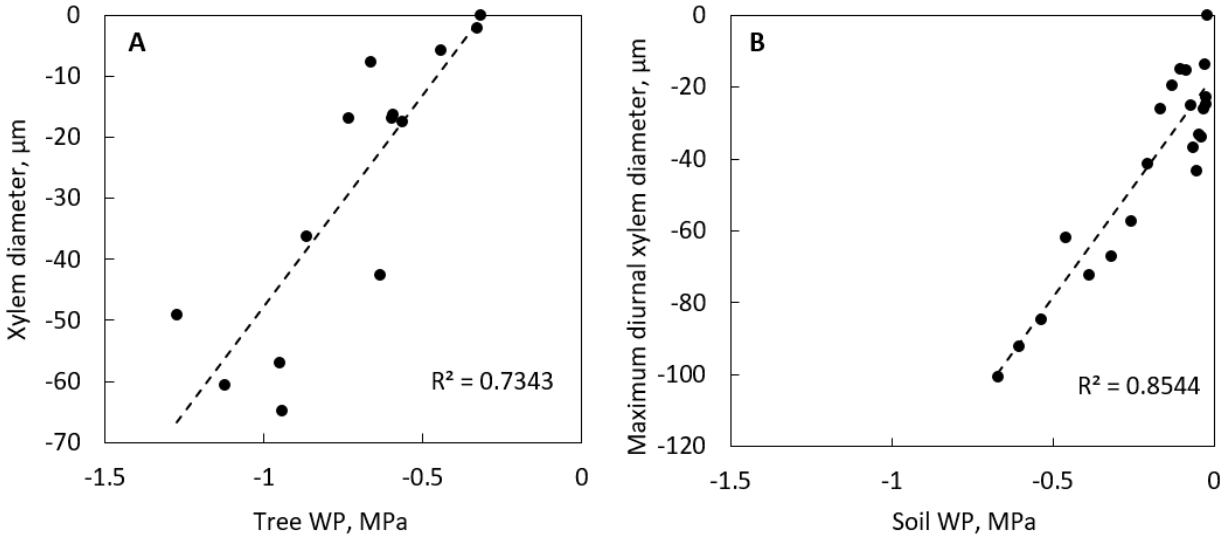

Fig. 1

$k_{bg} = \frac{F_{max}}{\Psi_s - \Psi_{stem\_min}}$, $k_{bg,d} = \frac{F_{max}}{dx_{max} - dx_{min}} = \frac{F_{max}}{\Delta dx}$

$g_s = \frac{F_{max}}{D_{max}}$

k_{bg} is soil-to-stem hydraulic conductance
$k_{bg,d}$ is proxy for soil-to-stem hydraulic conductance
F_{max} is maximum daily sap flow rate
Ψ_s is soil water potential
Ψ_{stem_min} is minimum daily stem water potential
dx_{max} is maximum daily xylem diameter*
dx_{min} is minimum daily xylem diameter*
Δdx is daily amplitude of diameter change
g_s is canopy conductance at maximum water use
D_{max} is maximum daily VPD

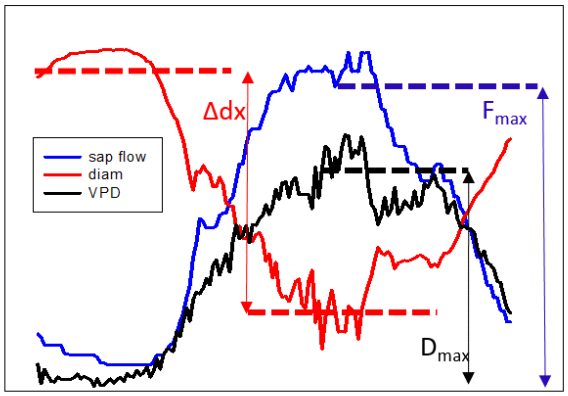

**delta in the diameter measurement notations refers to a change compared to a reference state, not change in time*

Fig. 2

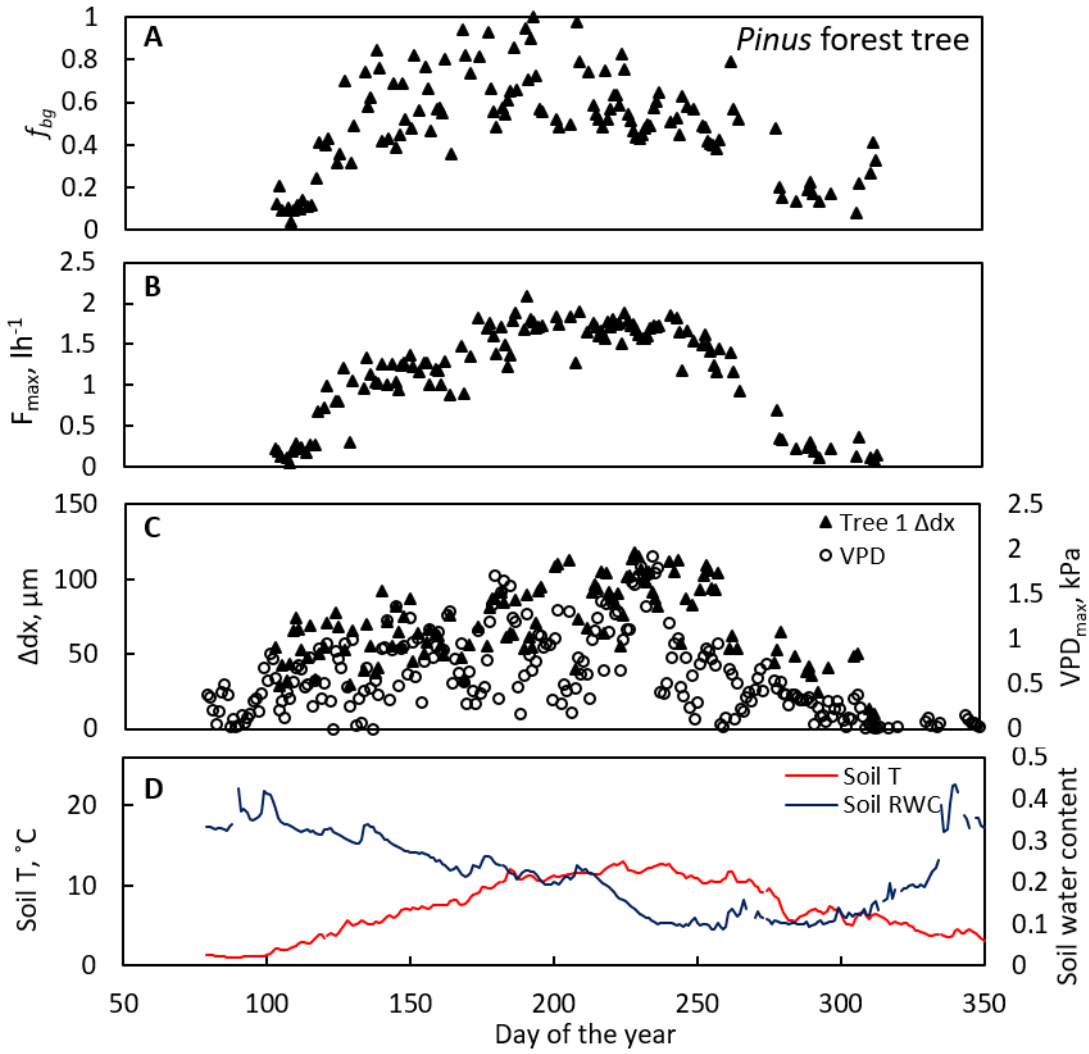
A
Pinus forest tree
f_{bg}
B
F_{max}, lh^{-1}
C
Tree 1 Δdx
VPD
Δdx, µm
VPD$_{max}$, kPa
D
Soil T
Soil RWC
Soil T, °C
Soil water content
Day of the year

835

836 **Fig. 3**

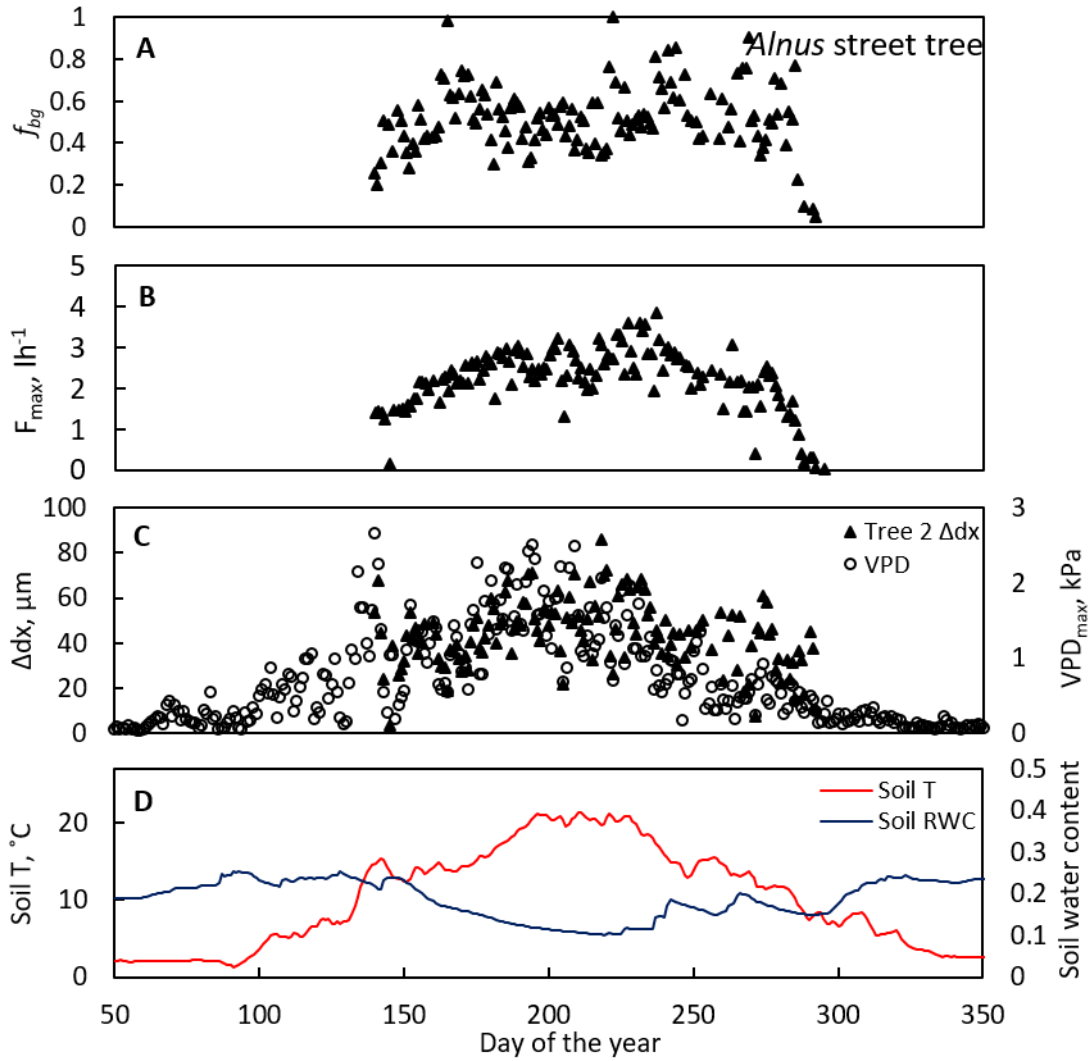
A
Alnus street tree
f_{bg}
B
F_{max}, lh^{-1}
C
Tree 2 Δdx
VPD
Δdx, µm
VPD$_{max}$, kPa
D
Soil T
Soil RWC
Soil T, °C
Soil water content
Day of the year

837

838 **Fig. 4**

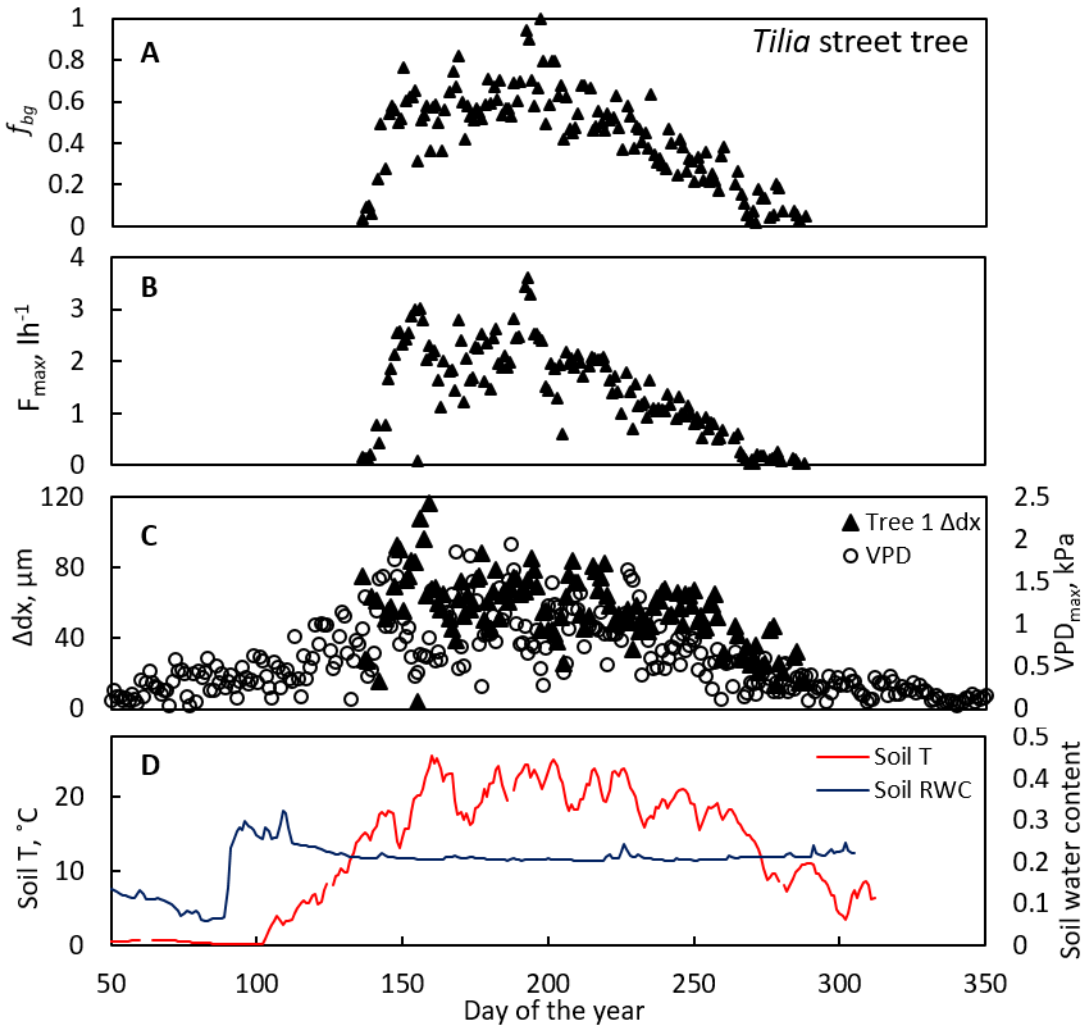
A
Tilia street tree
f_{bg}
B
F_{max}, lh^{-1}
C
Δdx, µm
Tree 1 Δdx
VPD
VPD_{max}, kPa
D
Soil T, °C
Soil T
Soil RWC
Soil water content
Day of the year

839

840 **Fig. 5**

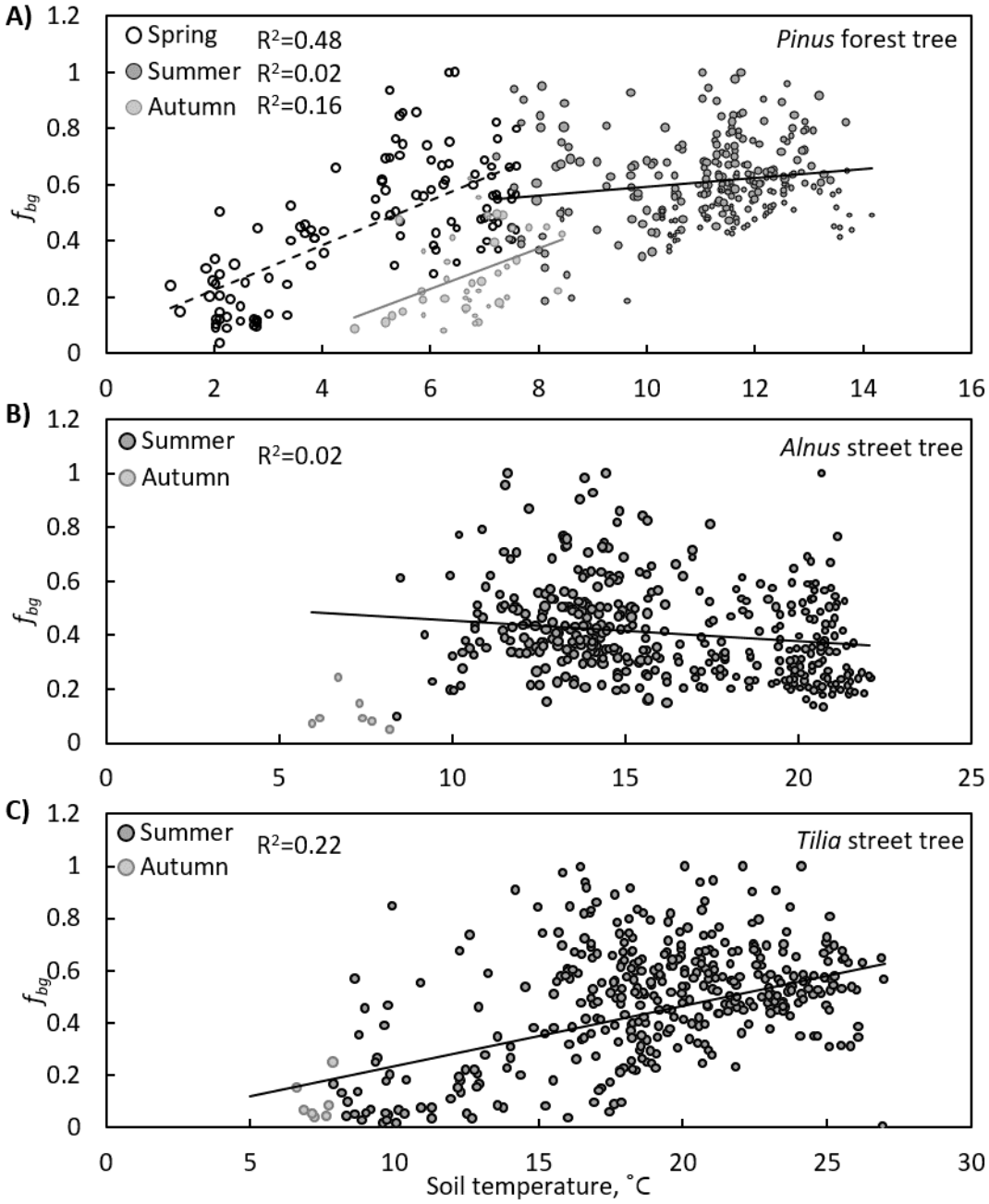
A)
Spring
Summer
Autumn
R²=0.48
R²=0.02
R²=0.16
Pinus forest tree
B)
Summer
Autumn
R²=0.02
Alnus street tree
C)
Summer
Autumn
R²=0.22
Tilia street tree
f_{bg}
Soil temperature, ˚C

841

842 **Fig. 6**

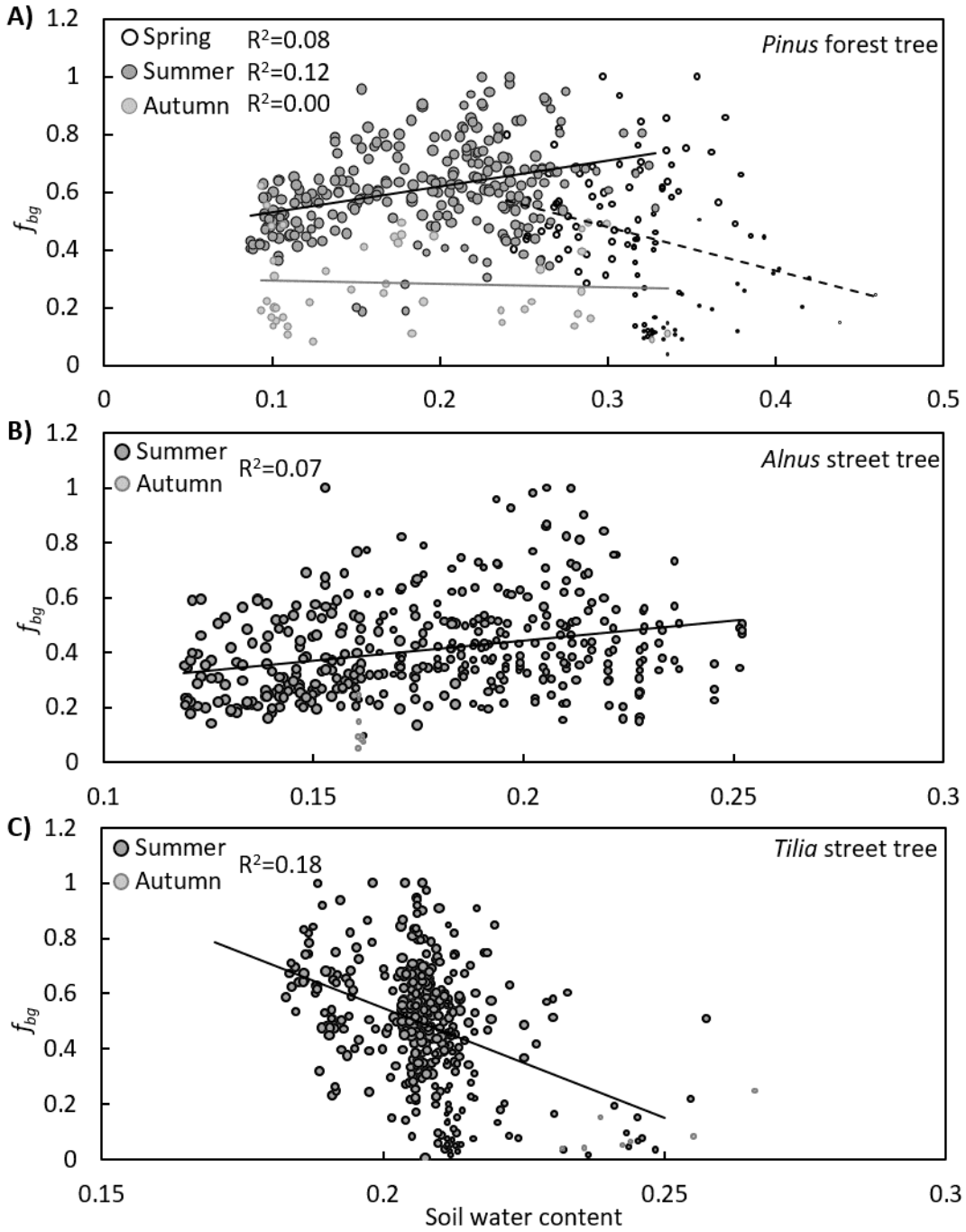
A)
Spring R²=0.08
Summer R²=0.12
Autumn R²=0.00
Pinus forest tree
B)
Summer
Autumn R²=0.07
Alnus street tree
C)
Summer
Autumn R²=0.18
Tilia street tree
f_{bg}
Soil water content

843

844 **Fig. 7**

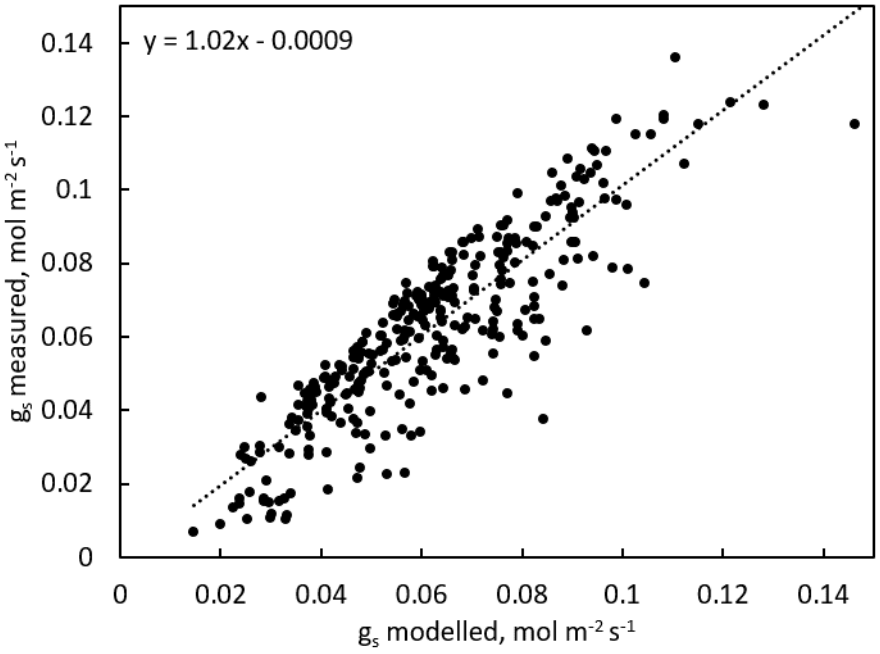
y = 1.02x - 0.0009
0.14
0.12
0.1
0.08
0.06
0.04
0.02
0
g_s measured, mol m^{-2} s^{-1}
0
0.02
0.04
0.06
0.08
0.1
0.12
0.14
g_s modelled, mol m^{-2} s^{-1}

845

846 **Fig. 8**